Cellular/Molecular

Constitutive and Synaptic Activation of GIRK Channels Differentiates Mature and Newborn Dentate Granule Cells

Jose Carlos Gonzalez,[1] S. Alisha Epps,[2] Sean J. Markwardt,[1] Jacques I. Wadiche,[1] and Linda Overstreet-Wadiche[1]
Departments of [1]Neurobiology and [2]Physical Medicine and Rehabilitation, University of Alabama at Birmingham, Birmingham, Alabama 35294

Sparse neural activity in the dentate gyrus is enforced by powerful networks of inhibitory GABAergic interneurons in combination with low intrinsic excitability of the principal neurons, the dentate granule cells (GCs). Although the cellular and circuit properties that dictate synaptic inhibition are well studied, less is known about mechanisms that confer low GC intrinsic excitability. Here we demonstrate that intact G protein-mediated signaling contributes to the characteristic low resting membrane potential that differentiates mature dentate GCs from CA1 pyramidal cells and developing adult-born GCs. In mature GCs from male and female mice, intact G protein signaling robustly reduces intrinsic excitability, whereas deletion of G protein-activated inwardly rectifying potassium channel 2 (GIRK2) increases excitability and blocks the effects of G protein signaling on intrinsic properties. Similarly, pharmacological manipulation of $GABA_B$ receptors ($GABA_B$Rs) or GIRK channels alters intrinsic excitability and GC spiking behavior. However, adult-born new GCs lack functional GIRK activity, with phasic and constitutive $GABA_B$R-mediated GIRK signaling appearing after several weeks of maturation. Phasic activation is interneuron specific, arising primarily from nNOS-expressing interneurons rather than parvalbumin- or somatostatin-expressing interneurons. Together, these results demonstrate that G protein signaling contributes to the intrinsic excitability that differentiates mature and developing dentate GCs and further suggest that late maturation of GIRK channel activity is poised to convert early developmental functions of $GABA_B$ receptor signaling into $GABA_B$R-mediated inhibition.

Key words: **adult neurogenesis; dentate gyrus; G protein; $GABA_B$; GABAergic; interneuron**

Significance Statement

The dentate gyrus exhibits sparse neural activity that is essential for the computational function of pattern separation. Sparse activity is ascribed to strong local inhibitory circuits in combination with low intrinsic excitability of the principal neurons, the granule cells. Here we show that constitutive activity of G protein-coupled inwardly rectifying potassium channels (GIRKs) underlies to the hallmark low resting membrane potential and input resistance of mature dentate neurons. Adult-born neurons initially lack functional GIRK channels, with constitutive and phasic $GABA_B$ receptor-mediated GIRK inhibition developing in tandem after several weeks of maturation. Our results reveal that $GABA_B$/GIRK activity is an important determinant of low excitability of mature dentate granule cells that may contribute to sparse DG activity *in vivo*.

Introduction

The dentate gyrus (DG) is a main entry point for neural activity into the hippocampal formation, integrating sensory and spatial information from the cortex in a manner that generates a neural representation of a context (Hernández-Rabaza et al., 2008; Liu et al., 2014). The DG exhibits sparse neural activity wherein only a small fraction of the principal granule cells (GCs) are active at any given time and active GCs have generally low firing rates (Jung and McNaughton, 1993; Chawla et al., 2005; Leutgeb et al., 2007; Neunuebel and Knierim, 2012). Sparse population and rate coding are essential components of the computational function of pattern separation wherein similar input patterns are transformed into distinct output patterns and also underlie the DG "gate" that suppresses the transmission of epileptiform activity (Coulter and Carlson, 2007; Hsu, 2007; Treves et al., 2008). It is widely acknowledged that strong networks of GABAergic in-

Received March 13, 2018; revised May 30, 2018; accepted May 30, 2018.

Author contributions: J.C.G., S.A.E., S.J.M., J.I.W., and L.O.-W. designed research; J.C.G., S.A.E., and S.J.M. performed research; J.C.G., S.A.E., and S.J.M. analyzed data; J.C.G. and L.O.-W. wrote the paper.

This work was supported by National Institutes of Health (NIH) Grants RO1-NS-064025 (L.O.-W.) and RO1-NS-065920 (J.I.W.). S.A.E. and L.O.-W. were also supported by NIH Grant RO1-NS-075162. We thank Candace L. Floyd for helpful comments and the financial support of S.A.E. and L.O.-W through NIH Grant RO1-NS-075162. We also thank members of the Wadiche laboratories for helpful comments throughout this project, Mary Seelig for technical assistance, and Drs. Karen Gamble and John Hablitz for sharing mouse lines.

The authors declare no competing financial interests.

Correspondence should be addressed to either Dr. Jacques I. Wadiche or Dr. Linda Overstreet-Wadiche, UAB Department of Neurobiology, 1825 University Boulevard, Birmingham, AL 35294, E-mail: jwadiche@uab.edu or lwadiche@uab.edu.

S.A. Epps's present address: Department of Psychology, Whitworth University, Spokane, WA 99251.

S.J. Markwardt's present address: Avant Healthcare, Carmel, IN 46032.

DOI:10.1523/JNEUROSCI.0674-18.2018
 0270-6474/18/386513-14$15.00/0

terneurons in combination with the low intrinsic excitability of GCs enforce sparse DG activity. Whereas $GABA_A$-receptor-mediated inhibition is widely studied, less is known about the role of $GABA_B$ receptors ($GABA_B$Rs) and mechanisms underlying the low intrinsic excitability of GCs.

$GABA_B$Rs are $G_{i/o}$ coupled metabotropic receptors with both presynaptic and postsynaptic actions that are mediated by distinct receptor subunits and effector pathways (Pinard et al., 2010). The activation of postsynaptic $GABA_B$Rs dissociates $G\beta\gamma$ from $G\alpha$ to directly gate G protein-coupled inwardly rectifying potassium (GIRK) channels, leading to a slow hyperpolarizing conductance (Andrade et al., 1986; Dutar and Nicoll, 1988; Solís and Nicoll, 1992; De Koninck and Mody, 1997; Lüscher et al., 1997). The nonuniform distribution of $GABA_B$R subunits and, in particular, GIRK channels generates a laminar distribution of $GABA_B$R-mediated current densities across the somatodendritic domain of principal neurons (Kulik et al., 2006; Degro et al., 2015). $GABA_B$Rs are located extrasynaptically and are thus typically activated by GABA spillover, resulting either from repetitive synaptic activity or the activation of specific interneurons that mediate a form of volume transmission (Otis and Mody, 1992; Otis et al., 1993; Fritschy et al., 1999; Scanziani, 2000; Tamás et al., 2003; Price et al., 2008; Armstrong et al., 2011). Hence, slow $GABA_B$-mediated phasic inhibition is constrained by the accessibility of postsynaptic receptors to synaptically released GABA. In contrast, constitutive opening of GIRK channels, either by agonist-independent spontaneous GTP/GDP turnover or persistent activation of $G_{i/o}$-coupled metabotropic receptors can contribute to steady-state dendritic excitability and resting membrane potential (RMP) in some neural populations (Breitwieser and Szabo, 1988; Lüscher et al., 1997; Chen and Johnston, 2005; Kim and Johnston, 2015).

In addition to controlling GC excitability, GABA acts as a trophic factor during the maturation of adult-born GCs, during which newly generated GCs transition from high to low intrinsic excitability (Schmidt-Hieber et al., 2004; Mongiat et al., 2009; Dieni et al., 2013a,b; Brunner et al., 2014). Young GCs express low levels of inwardly rectifying potassium (K_{ir}) channels and overexpression of K_{ir} 2.1 in young neurons can induce mature repetitive firing characteristics, suggesting that K_{ir} channels contribute to mature GC intrinsic excitability (Mongiat et al., 2009). Indeed, mature GCs express many types of potassium channels that contribute to intrinsic excitability (Beck et al., 1992, 1997; Rüschenschmidt et al., 2006; Kirchheim et al., 2013), but the origin of the unusually low RMP of GCs is unclear. Here we investigate the contribution of GIRK channels to the excitability of mature and adult-born GCs. GIRK channels function in a complex with $GABA_B$Rs (Wang et al., 2016), and both are highly expressed in the DG with presynaptic and postsynaptic functions (Mott and Lewis, 1992; Otis and Mody, 1992; Mott et al., 1993, 1999; Otis et al., 1993; Brucato et al., 1995; Canning and Leung, 2000; Foster et al., 2013; Degro et al., 2015). We focus on postsynaptic signaling to assess the function, maturation, and sources of $GABA_B$/GIRK signaling in dentate GCs.

Materials and Methods

Animal and experimental procedures. To identify newly generated adult-born GCs, we used reporter mice with enhanced green fluorescent protein (EGFP) expressed under the control of the proopiomelanocortin (POMC) promoter (POMC-EGFP; Cowley et al., 2001; Overstreet et al., 2004), or GFP expressed under the control of the glutamate decarboxylase isoform 67 (GAD67-GFP; Zhao et al., 2010). We also used Nestin-CreER^{TM4} mice (provided by C. Kuo (Duke University, Durham, NC); Kuo et al., 2006) crossed with Ai14 R26R-TdTomato reporter mice (stock #007914, The Jackson Laboratory) to identify adult-born GCs between 3 and 5 weeks post-tamoxifen induction. EGFP, GFP, or td-Tomato-expressing GCs were identified using epifluorescence illumination, with comparisons to unlabeled neighboring mature GCs. GIRK2 knock-out (KO) mice were also used (Signorini et al., 1997). Optogenetic activation of interneuron subtypes was performed by crossing neuronal nitric oxide synthase (nNOS)-CreER (stock #014541, The Jackson Laboratory), PV^{Cre} (stock #008069, The Jackson Laboratory), or SOM-IRES-Cre (stock #013044, The Jackson Laboratory) mice with Ai32 channelrhodopsin 2 (ChR2)/enhanced yellow fluorescent protein (EYFP) mice (stock #012569, The Jackson Laboratory). Positive offspring were identified by PCR. Inducible Cre mice were fed with tamoxifen pellets *ad libitum* (Envigo) for 7 d after weaning at postnatal day 22. Experiments were performed with male and female 7- to 10-week-old mice derived from different lines maintained on the C57BL/6J background, with the exception of Nestin-CreER mice, which were maintained on a CD1 background. No significant differences in mature GC properties were detected between different mouse lines, so data were pooled. All animal procedures followed the *Guide for the Care and Use of Laboratory Animals*, US Public Health Service, and were approved by the University of Alabama at Birmingham Institutional Animal Care and Use Committee. Mice were maintained in standard housing in a 12 h light/dark cycle and recordings were performed between zeitgeber time 7 (ZT7) and ZT11.

Slice preparation. Mice were preanesthetized with isoflurane, deeply anesthetized with 2,2,2-tribromoethanol (Avertin; Sigma-Aldrich), and perfused intracardially with ice-cold modified ACSF containing the following (in mM): 110 choline chloride, 25 D-glucose, 7 $MgCl_2$, 2.5 KCl, 1.25 Na_2PO_4, 0.5 $CaCl_2$, 1.3 Na-ascorbate, 3 Na-pyruvate, and 25 $NaHCO_3$, bubbled with 95% O_2/5% CO_2. The brain was removed and 300-μm-thick horizontal slices were prepared using a vibratome (VT1200S, Leica Instruments). Slices were incubated at 37°C for ~30 min in recording solution containing the following (in mM): 125 NaCl, 2.5 KCl, 1.25 Na_2PO_4, 2 $CaCl_2$, 1 $MgCl_2$, 25 $NaHCO_3$, and 25 D-glucose bubbled with 95% O_2/5% CO_2, then transferred to room temperature in the same solution.

Electrophysiology. Slices were mounted on a BX51WI Olympus microscope and superfused with recording solution. For whole-cell recordings, patch pipettes were filled with the following (in mM): 135 K-gluconate, 3 KCl, 2 $MgCl_2$, 10 HEPES, 2 Mg-ATP, 0.5 Na-GTP, 10 phosphocreatine, and 0.1 EGTA, pH 7.3 and 310 mOsm (GTP^+). When noted, 0.5 Na-GTP was excluded from the same internal solution (GTP^-). To confirm the integrity of the patch in perforated-patch recordings, and for whole-cell $GABA_A$ IPSC recordings associated with Figure 7, we used a high $[Cl^-]$ intracellular solution containing the following (in mM): 140 KCl, 4 $MgCl_2$, 10 HEPES, 4 Mg-ATP, 0.3 Na-GTP 7 phosphocreatine, 10 EGTA, 50–100 μg/ml gramicidin, and 0.2–0.4% DMSO (since EGTA is too large to permeate gramicidin pores, it is likely irrelevant for results using perforated patch recordings).

Electrophysiological recordings were made with fire-polished borosilicate glass electrodes (outer diameter, 1.5 mm, inner diameter, 0.86 mm; Sutter Instrument) with resistance of 2–5 MΩ for mature GCs and 4–7 MΩ for immature GCs when filled with the intracellular solution. Pipettes were mounted on the headstage (CV-7B) of a 700A amplifier (Molecular Devices) with cancellation of pipette capacitive transients. Bridge balance was automatically adjusted in current-clamp recordings, and action potential threshold was detected at rheobase when the slope exceeded 10 mV/ms. In voltage clamp, membrane potential was held at −70 mV to generate a standing outward potassium current. Holding currents were measured by averaging the amplitude of baseline currents for 20 s or in five different sweeps in each condition. Measures of intrinsic excitability were obtained starting 5–10 min after cell break-in, based on the time required for us to block synaptic-activated $GABA_B$/GIRK coupling in distal dendrites using an intracellular solution containing QX-314 (Hibino et al., 2010), and only cells with stable measures over the course of the experiment were included. Most recordings were made at 30°C, although some were made at 22°C (as noted). Series resistance was uncompensated (<25 MΩ), and experiments were discarded if substan-

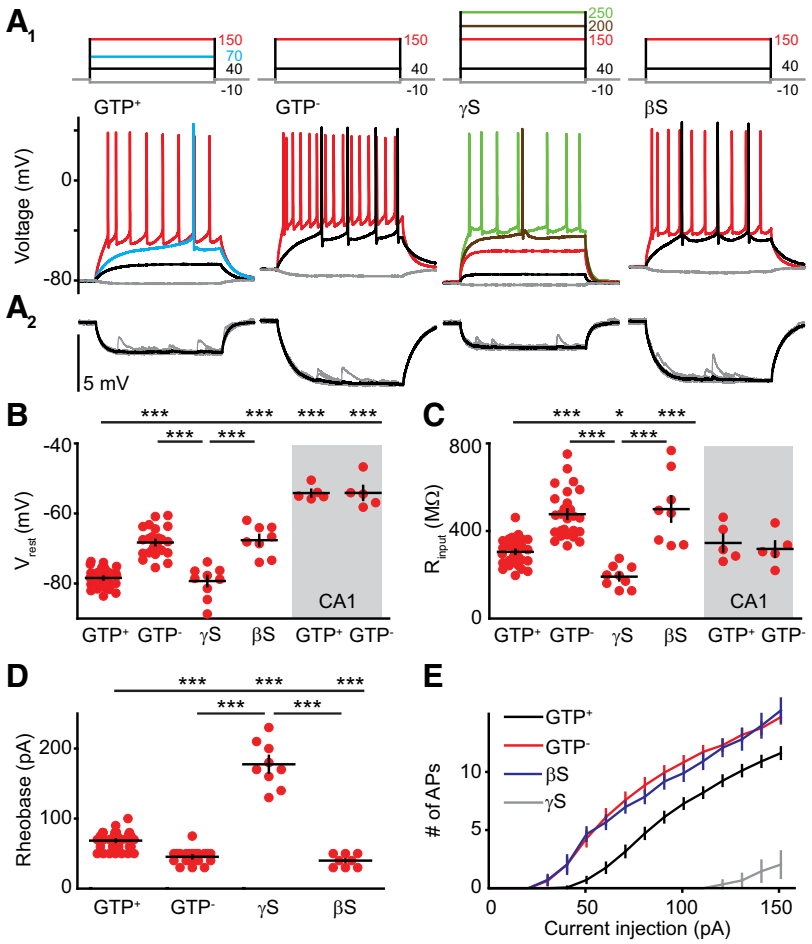

Figure 1. Intact G protein signaling is required for low GC intrinsic excitability. ***A*$_1$**, Top, Current injections (500 ms) used to measure GC intrinsic excitability with different intracellular solutions. Bottom, Voltage responses with color indicating current injections shown above. ***A*$_2$**, Enlarged voltage response evoked by a 10 pA hyperpolarizing current injection used to calculate input resistance. Average of 50 traces in black. ***B–D***, Comparison of properties from GCs and CA1 pyramidal cells. ***B*** shows (from left to right) RMP from 38, 26, 9, and 8 GCs, and 5 and 5 CA1 pyramidal cells (shaded area) recorded with the internal shown below. ***Top bar showing differences vs GTP$^+$. Differences between CA1 cells and GCs not shown (see Results). ANOVA, $F_{(5,85)} = 99.63$. ***C*** shows input resistance from the same cells as ***B***. ANOVA, $F_{(5,85)} = 20.24$. ***D*** shows the current threshold to elicit the first spike for the GCs in ***B***. ANOVA, $F_{(3,71)} = 172.1$. ***E***, Number of spikes elicited by increasing current steps measured during 500 ms. GTP$^+$, $n = 27$; GTP$^-$, $n = 16$; GTPγS. $n = 9$; GDPβS, $n = 7$. Data are the mean ± SEM (lines) and individual values (symbols). Bonferroni's *post hoc* test: ***$p < 0.001$; **$p < 0.01$; *$p < 0.05$.

tial changes (>15%) were observed. Voltages were not corrected for junction potentials, calculated to be 13.6 mV. Currents were filtered at 2 kHz and sampled at 10 kHz (MultiClamp 700A; Molecular Devices). Input resistance (IR) was obtained from hyperpolarizing current injections of 2–10 pA at resting potential. Synaptic stimulation was achieved using a constant-current stimulator (Digitimer) and a patch pipette filled with recording solution placed in mid-molecular layer (100 μs; 200 μA). Light stimuli (1 ms) were delivered using a T-Cube LED Driver (LEDD1B, Thor Laboratories) mounted in the epifluorescence light path of a BX51WI Olympus microscope. Data were analyzed with Axograph X (Axograph Scientific) and Clampfit (Molecular Devices). Drugs and chemicals were obtained from Sigma-Aldrich, Tocris Bioscience, or Ascent Scientific.

Immunohistochemistry. Confocal images were taken of POMC-EGFP, GAD67-GFP, and Neston-CreER^{TM4} × Ai14 immature GCs; nNOS, somatostatin (SST), and parvalbumin (PV) × Ai32 interneurons (50 μm sections both conditions); and from biocytin-filled GCs in 300 μm slices after overnight fixation, as described previously (Chancey et al., 2013). Sections were immunostained with Alexa Fluor-488-conjugated anti-GFP (1:1000) or Alexa Fluor-568 (1:800)-conjugated anti-DsRed (1:400) and imaged using a 20× water-immersion objective mounted on an Olympus FV1200 Confocal Microscope using z steps of 1 μm. Alexa Fluor-647-conjugated streptavidin (1:3000) was used for biocytin reconstructions. Relative fluorescence was measured using a 160 × 30 pixel area from maximum z-projections (ImageJ, National Institutes of Health).

Experimental design and statistical analysis. We pooled a large number of mature GC recordings across intracellular solutions and mouse lines to have a reference for population values of RMP and input resistance that is indicated in some figures as dotted lines. Data are expressed as mean ± SEM, and, unless noted, one-way ANOVAs were used to determine statistical significance at $p < 0.05$. Normality and variance were tested before analysis. *Post hoc* analyses were made with Bonferroni's or Tukey's tests. In some cases, within-cell comparisons to assess pharmacological manipulations used paired t tests with statistical significance at $p < 0.05$. Statistical analyses were performed using Prism (GraphPad Software).

Results

Intact G protein signaling is required for low GC intrinsic excitability

A hallmark of dentate GCs is the negative RMP that differentiates GCs from hippocampal pyramidal cells (Spruston and Johnston, 1992). The mechanism underlying the hyperpolarized RMP is unknown but is expected to involve a specific complement of potassium channels that comprise the resting membrane conductance (Mongiat et al., 2009; Young et al., 2009; Yarishkin et al., 2014). We noted that prior studies using whole-cell recordings that include GTP in the intracellular solution typically report more hyperpolarized values compared with those without GTP (Otis and Mody, 1992; Staley and Mody, 1992; Otis et al., 1993; Liu et al., 1996; Overstreet et al., 2004; Schmidt-Hieber et al., 2004, 2007; Laplagne et al., 2006; Mongiat et al., 2009; Young et al., 2009; Ewell and Jones, 2010; Tanner et al., 2011; Chiang et al., 2012; Brunner et al., 2013, 2014; Dieni et al., 2013b, 2016; Pernía-Andrade and Jonas, 2014; Heigele et al., 2016; Kowalski et al., 2016). Thus, we tested how G protein-mediated signaling affects the intrinsic properties of GCs by targeting mature GCs located in the mid-granular to outer-granular cell layer for whole-cell recordings using a potassium gluconate-based internal solution with or without GTP (0.5 mM). We found that the presence of GTP in the pipette produced a negative shift in the RMP of ~10 mV (Fig. 1*A*,*B*; GTP$^+$, −78 ± 0.4 mV; GTP$^-$, −68 ± 0.7 mV). When we accounted for the calculated liquid junction potential of our internal solution (13.6 mV), the RMP in whole-cell recordings with GTP in the pipette was similar to the RMP in gramicidin perforated patch recordings in which there is expected to be only a small Donnan potential (−87 ± 2.4 mV; Mann–Whitney test, $p = 0.003$ without correction; $p = 0.08$ with correction; $n = 7$, data not shown). In whole-cell recordings, we made small current injections (−10 pA) to test the input resistance near RMP and

found that the hyperpolarized RMP with GTP was associated with a 65% reduction in input resistance (Fig. 1*A*,*C*; 310 ± 9 vs 477 ± 21 MΩ). The difference in input resistance did not result from the shift in RMP, since a similar difference in input resistance was detected in a subset of cells that were also measured at −70 mV (data not shown). In contrast, CA1 pyramidal cells had a more depolarized RMP than GCs, and neither RMP nor input resistance was affected by the presence of 0.5 mM GTP in the pipette (GTP^+: −54 ± 0.9 mV and 345 ± 38 MΩ; GTP^-: −54 ± 4 mV and 318 ± 35 MΩ). Together, these results suggest that intracellular GTP is required to maintain the low RMP and input resistance that is characteristic of dentate GCs.

To further probe the role of G protein-mediated signaling in GC intrinsic properties, we manipulated G protein activity using GTPγS (γS), a nonhydrolyzable GTP analog (500 μM) that confers constitutive G protein activity and GDPβS (βS), a nonhydrolyzable GDP analog (500 μM) that prevents G protein activity. The addition of γS to the GTP^- internal solution replicated the effects of GTP on the RMP (−79 ± 1.5 mV; Fig. 1*A*,*B*) and reduced the input resistance below the resistance of GTP alone (191 ± 17 MΩ; Fig. 1*A*,*C*). Conversely, when βS was included in GTP^+ internal solution, both the RMP and input resistance were similar to what was observed with GTP^- internal solution (−67 ± 1.5 mV; 500 ± 57 MΩ; Fig. 1*A*–*C*). In the same cells, we examined action potential firing in response to step current injections and found that the effects of GTP-mediated signaling on passive membrane properties translated into robust alterations in spiking behavior (Fig. 1*D*,*E*). Activation of the GTP system by the inclusion of GTP or γS increased rheobase (68 ± 2 and 176 ± 10 pA, respectively) and shifted the spike–current relationship to the right compared with exclusion of GTP or the inclusion of βS (rheobase = 45 ± 2 and 40 ± 4 pA, respectively). This change in rheobase reflects the importance of the input resistance to intrinsic excitability since alterations in G protein signaling did not affect the maximum action potential (AP) frequency (35 ± 1, 39 ± 2, 37 ± 3, 33 ± 2 Hz in GTP^+, GTP^-, βS and γS respectively; $F_{(3,42)} = 1.01$; $p = 0.39$) or the threshold for spiking (GTP^+, −40 ± 1 mV; GTP^-, −40 ± 1 mV; βS, −40 ± 1 mV; γS −39 ± 2 mV; $F_{(3,59)} = 0.24$; $p = 0.86$). Together, these results show that intact G protein-mediated signaling reduces the intrinsic membrane excitability of mature GCs by hyperpolarizing the RMP and reducing the input resistance.

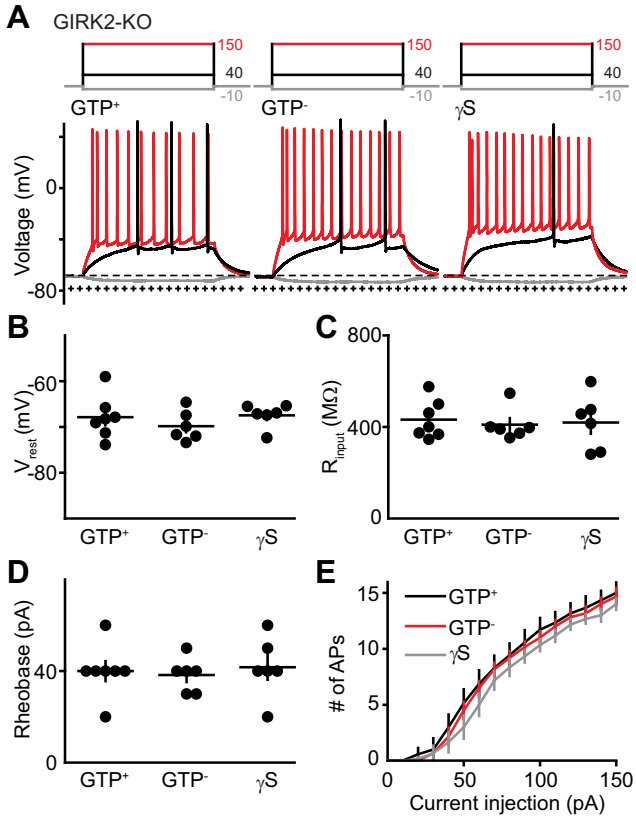

Figure 2. GC excitability is insensitive to intracellular GTP in GIRK2-KO mice. ***A***, Current injections (top, 500 ms) and voltage responses (bottom) in GCs from GIRK2 KO mice with the indicated intracellular solutions. Dotted + and − lines represent the average RMP of GTP^+ and GTP^- conditions in WT mice. ***B–D***, RMP, input resistance, and rheobase recorded in GIRK2 KO mice. ANOVA, $F_{(3,16)} = 0.71$; ANOVA, $F_{(3,16)} = 0.09$; ANOVA, $F_{(3,16)} = 0.81$, respectively. ***E***, Number of APs evoked by increasing current injections measured over 500 ms. GTP^+, $n = 7$; GTP^-, $n = 6$; γS, $n = 6$. Data are the mean ± SEM.

Constitutively active GIRKs mediate effects of GTP

GTP-dependent membrane hyperpolarization associated with decreased input resistance suggested the involvement of GIRK channels, a family of K_{ir} channels composed of homotetrameric or heterotetrameric complexes of GIRK1–4 subunits (for review, see Hibino et al., 2010; Lüscher and Slesinger, 2010). In CA1 pyramidal cells, millimolar levels of intracellular GTP can generate constitutive (receptor-independent) GIRK activation that hyperpolarizes the RMP (Lüscher et al., 1997). We thus wondered whether submillimolar GTP, which had no effect on CA1 pyramidal cells (Fig. 1*B*,*C*), affected RMP and the input resistance of GCs via GIRK channel activation. First, we tested GIRK2 germline KO mice, which have previously been shown to lack synaptic and constitutive GIRK channel activation in CA1 and locus ceruleus (Lüscher et al., 1997; Torrecilla et al., 2002). GCs in GIRK2 KO mice had similar RMPs (−68 ± 2 mV), input resistance (433 ± 32 MΩ), and rheobase (40 ± 4 pA) as GCs in WT mice when GTP was excluded from the internal solution, and in contrast to what we observed in WT GCs, these measures were unaffected by the inclusion of GTP or γS in the internal solution (Fig. 2*A*–*C*). Although G protein-mediated signaling can affect a variety of effectors, these results show that constitutive GIRK channel activity can fully explain the effect of GTP on the RMP, input resistance, and rheobase of mature GCs. However, since genetic deletion of GIRK2 also reduces GIRK1 levels (Signorini et al., 1997; Torrecilla et al., 2002), these results do not resolve the GIRK subunit specificity of GTP signaling.

To further probe the identity of channels that contribute to GC intrinsic excitability, we tested blockers of GIRKs in GIRK2 KO and WT mice. Ba^{2+} is a well known blocker of GIRKs and other K_{ir} channels (French and Shoukimas, 1985; Harnett et al., 2013). Consistent with constitutive activation of GIRKs in the presence of intracellular GTP, bath application of Ba^{2+} (500 μM) depolarized GCs (−61 ± 1.6 mV) and robustly increased input resistance (996 ± 70 MΩ; Fig. 3*A*–*D*). Ba^{2+} dramatically increased GC excitability (rheobase, 12 ± 1.6 pA), likely reflecting the additional contribution of blocking other K_{ir} channels (Mongiat et al., 2009). The GIRK1/4-selective blocker tertiapin-Q (TQ; 200 nM; Jin and Lu, 1999) increased the input resistance of GCs recorded with GTP-containing solution (from 332 ± 44 to 420 ± 60 MΩ, $p = 0.01$, $n = 6$) but, unexpectedly, did not alter RMP (−79 ± 1.3 vs −78 ± 0.8 mV; $p = 0.31$) or rheobase (from 65 ± 5.6 to 55 ± 9.6 pA; $p = 0.11$, $n = 6$; data not shown). In contrast, the GIRK1-selective activator ML297 (10 μM; Kaufmann et al., 2013; Wydeven et al., 2014) both hyperpolarized the RMP and reduced the input resistance to below basal levels in a GTP-

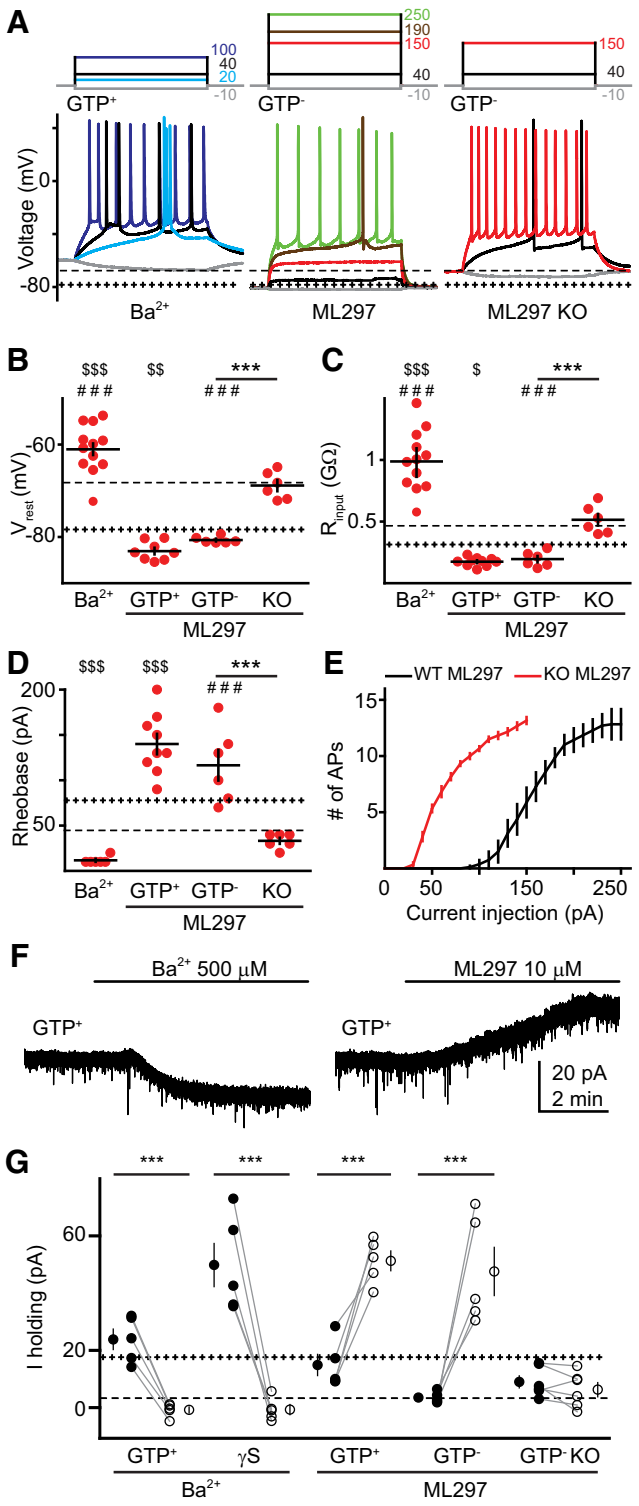

Figure 3. GIRK modulators affect mature GC intrinsic properties. ***A***, Current injections (top, 500 ms) and voltage responses (bottom) in GCs with the indicated intracellular solution and Ba^{2+} (500 μM) or ML297 (10 μM). Right, ML297 had no effect on GCs from GIRK2 KO mice. Dotted + and − lines represent mean values from GTP^+ and GTP^- conditions shown in Figure 1, respectively. ***B–D***, Individual (red) and mean (black) values of RMP (***B***), input resistance (***C***), and rheobase (***D***) recorded in GCs perfused with Ba^{2+} (GTP^+) or ML297 (GTP^+, GTP^-, and GIRK2 KO mice). ANOVA: $F_{(5,50)} = 62.28$, $F_{(5,51)} = 49.69$, and $F_{(5,50)} = 42.26$ for ***B–D***, respectively. Bonferroni's *post hoc* test: $^{***}p < 0.001$; $^{**}p < 0.01$; $^{*}p < 0.05$; $ indicate differences against GTP^+ pool; # indicate differences against GTP^-. ***E***, Number of APs evoked by increasing current injections measured over 500 ms after perfusing ML297 in WT and GIRK2 KO GCs ($n = 8$ and 6, respectively). ***F***, Representative currents (held at −70 mV) −70 mV) evoked by Ba^{2+} or ML297 using a GTP^+ intracellular solution. ***G***, The effect of Ba^{2+} or ML297 (open symbols) on outward currents (I holding) using the indicated internal solutions and GIRK2 KO mice. Dotted + and − lines represent mean standing outward current from 15 GCs using GTP^+ intracellular (18 ± 2 pA) and 11 GCs using GTP^- intracellular solution (4 ± 0.7 pA). Paired *t* test, $^{***}p < 0.001$. Single symbols represent the mean ± SEM and individual paired values are connected with lines.

independent manner (Fig. 3*A–D*). Moreover, ML297 did not have any effect on GC intrinsic properties from GIRK2 KO mice, confirming prior observations that KO of GIRK2 affects GIRK1 function (Fig. 3*A–E*). Together, these results show that GIRK1 subunit- and GIRK2 subunit-containing GIRK channels contribute to GC intrinsic excitability.

To measure the constitutive GIRK currents underlying the changes we observed in GC intrinsic excitability, we recorded the holding current in GCs voltage clamped at −70 mV (the average RMP without intact GTP signaling; Fig. 1). The outward standing current with GTP in the pipette (~20 pA) was blocked by Ba^{2+}, illustrating that this current was generated by constitutively open GIRK and K_{ir} channels (Fig. 3*F*, left). Inclusion of γS in the internal solution generated a larger standing outward current, presumably mediated by GIRK channels (since K_{ir} channels are insensitive to GTP), that was likewise blocked to the same level by Ba^{2+} (Fig. 3*G*). We also measured the outward current in WT GCs resulting from GIRK1 activation. ML297 increased the standing outward current (with and without GTP) to a similar level as the current induced by γS (Fig. 3*F*, right), whereas ML297 had no effect in GCs from GIRK2 KO mice (Fig. 3*G*), which are known to have low GIRK1 levels (Signorini et al., 1997; Torrecilla et al., 2002). Consistent with the lack of effect of TQ on the RMP, TQ did not alter the holding current in GTP conditions, although it blocked ~50% of the current induced by ML297 (data not shown), confirming that this concentration can reduce GIRK1-mediated currents. Together, these results show that a basal GIRK conductance contributes to mature GC excitability, which can be blocked or enhanced by manipulating GTP levels or by GIRK channel modulators. Whereas both GIRK1 and GIRK2 contribute to low input resistance, these results suggest that GIRK2 contributes to the low somatic RMP of GCs.

Constitutive GIRK activity does not require $GABA_B$ receptor activation

GIRK channel activity is typically initiated by G_i/G_o-coupled metabotropic receptors like $GABA_B$ receptors. In the DG, the tonic activation of $GABA_A$ receptors by ambient extracellular GABA contributes to the integrative properties of GCs (Overstreet and Westbrook, 2001; Nusser and Mody, 2002; Wei et al., 2004; Mtchedlishvili and Kapur, 2006), suggesting that ambient GABA could also generate tonic $GABA_B$R-mediated GIRK channel activity. Alternatively, sufficient availability of $\beta\gamma$ subunits could allow constitutive GIRK channel activity that is independent of G_i/G_o-coupled metabotropic receptor ligands. To differentiate these possibilities, we tested $GABA_B$ receptor antagonists while also manipulating $\beta\gamma$ subunit availability.

First, we tested the effect of the selective $GABA_B$ receptor antagonist CGP55845 on the passive and active properties of mature GCs. In the presence of intracellular GTP, bath application of CGP55845 (10 μM) depolarized the RMP (from −79 ± 0.8 to −75 ± 0.8 mV) and increased the input resistance (from 320 ± 10 to 438 ± 12 MΩ). These changes in passive properties decreased rheobase (from 73 ± 2 to 40 ± 6 pA; $p = 0.001$, $n = 6$) and increased the number of spikes at low-current step injections

←

(Fig. 4*G*, left, middle left). As expected, the deactivation of the GTP system by removing GTP or adding βS to the intracellular solution occluded the effect of CGP55845 (Fig. 4*A*,*B*,*D*,*E*–*G*). These results initially suggested that constitutive $GABA_BR$ activation contributes to constitutive GIRK channel activity. However, we also tested the effect of CGP55845 when G protein-mediated signaling was enhanced by the nonhydrolyzable substrate GTPγS. Interestingly, CGP55845 had a similar effect on the RMP (from −79 ± 2 to 73 ± 3 mV) and input resistance (from 205 ± 22 to 429 ± 40 MΩ) as when we used GTP^+ internal solution (Fig. 4 *A*,*D*,*E*,*F*). The robust effect of intracellular γS on rheobase and spike number was likewise blocked by CGP55845 (Fig. 4*C*,*G*, middle right). While it was initially surprising that GIRK signaling produced by γS (i.e., downstream of $GABA_B$ receptors) was sensitive to $GABA_B$ receptor blockade, we note that CGP55845 is an inverse agonist that eliminates constitutive (ligand-independent) G protein signaling (Mukherjee et al., 2006; Riven et al., 2006). Thus, we next tested the competitive $GABA_B$ receptor antagonist CGP35348 (100 μM) using GTP in the pipette. In contrast to the inverse agonist, this pure antagonist had no effect on the RMP and spiking behavior and only a minor effect on the input resistance (Fig. 4*H*). Together, these results suggest that constitutive GIRK channel activity in mature GCs is primarily driven by the availability of βγ subunits that is independent of $GABA_BR$ activation by ambient GABA. In contrast, there was no effect of the $GABA_B$ receptor inverse agonist on RMP, input resistance, or spiking in CA1 pyramidal cells, with or without 0.5 mM GTP in the pipette (data not shown).

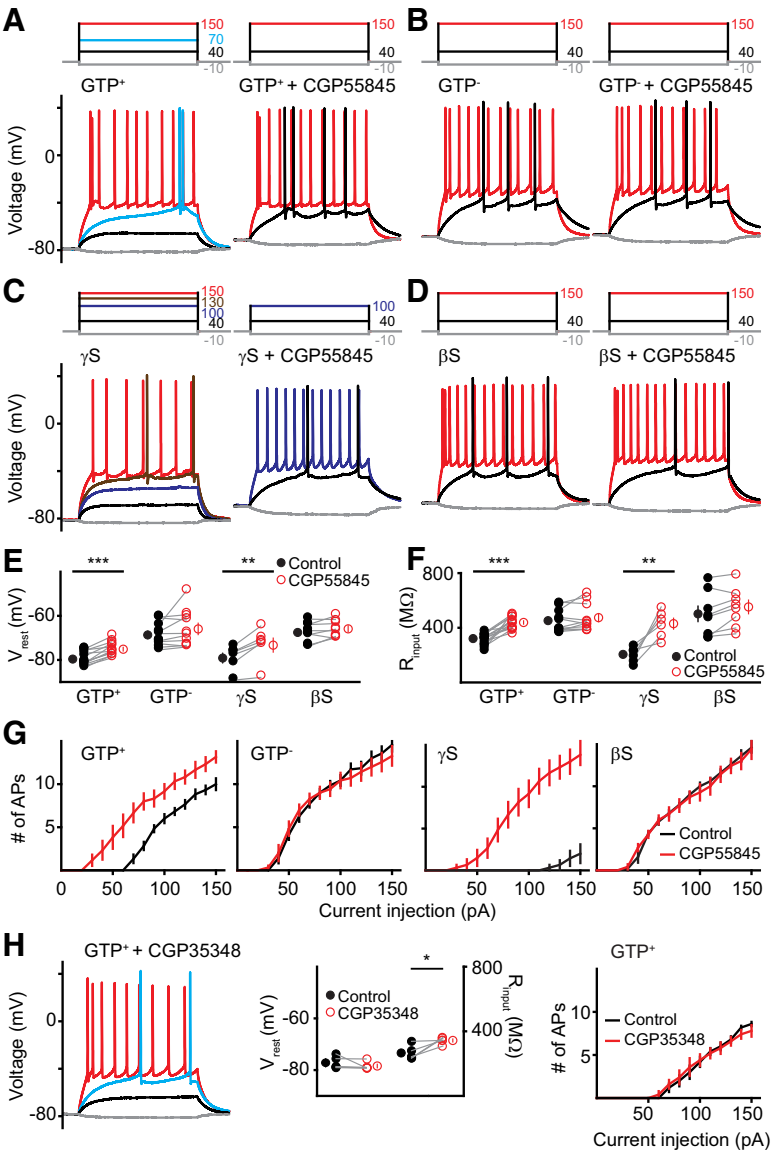

Figure 4. Constitutive GIRK activity does not require $GABA_B$ receptor activation. ***A–D***, Example current injections (top, 500 ms) and voltage traces (bottom) from GCs using GTP^+ (***A***), GTP^- (***B***), γS (***C***), or βS (***D***) before (left) and after (right) CGP55845 (10 μM). ***E***, ***F***, The inverse agonist CGP55845 increased the RMP (***E***) and input resistance (***F***) using GTP^+ or γS intracellularly. GTP^+, $n = 12$; GTP^-, $n = 10$; γS, $n = 6$; βS, $n = 8$. Paired *t* test: ***$p < 0.001$; **$p < 0.01$. ***G***, The number of APs evoked by increasing current injections in basal conditions (black) and after CGP55845 (red) measured over 500 ms. ***H***, Example voltage traces (left, color coded as in ***A***), RMP, and input resistance values (middle), and AP number (right) using the competitive $GABA_B$ receptor antagonist CGP35348 (100 μM). Statistical analysis: paired *t* test, *$p < 0.05$.

Newborn dentate GCs lack functional GIRK channels

Resident neural stem cells in the adult DG continuously generate new GCs that gradually acquire the intrinsic and synaptic properties of mature GCs over several weeks (Espósito et al., 2005; Dieni et al., 2013b; Toni and Schinder, 2015). A lack of functional K_{ir} channels contributes to the high intrinsic excitability and distinct spiking pattern of 3- to 4-week-old adult-born GCs (Mongiat et al., 2009). Thus, we wondered whether delayed function of GIRK channels likewise contributes to the high excitability of newly generated GCs. To address this question, we first used POMC-eGFP reporter mice to target newborn GCs at a homogeneous functional stage that occurs, on average, ~10–12 d postmitosis (Overstreet-Wadiche and Westbrook, 2006), and bath applied baclofen (30 μM) to generate $GABA_B$-mediated GIRK activation (Andrade et al., 1986). POMC-GFP-expressing newborn GCs had depolarized RMP reflected as a negative holding current in cells clamped at −70 mV and very high input resistance that was unaffected by baclofen (Fig. 5*B*, top left, top right). In contrast, baclofen induced a robust outward current and decrease of input resistance that was blocked by the inverse agonist CGP55845 beyond basal levels in neighboring mature GCs, consistent with constitutive activation (Fig. 5*A*). To further probe for small GIRK/K_{ir} contributions to the holding current of immature GCs at −70 mV, we bath applied Ba^{2+} or ML297 and generated all-point histograms fit with Gaussian distributions. Neither manipulation, even using γS in the internal solution, affected the holding current or fits of the current noise (Fig. 5*B*, bottom left, bottom right; paired *t* test: Ba^{2+}: $p = 0.51$, $n = 5$; ML297: $p = 0.57$, $n = 6$). Likewise, current-clamp recordings from POMC-GFP cells revealed that ML297 had no effect on the RMP (paired *t* test, $p = 0.44$; $n = 4$) or input resistance (paired *t* test, $p = 0.88$; data not

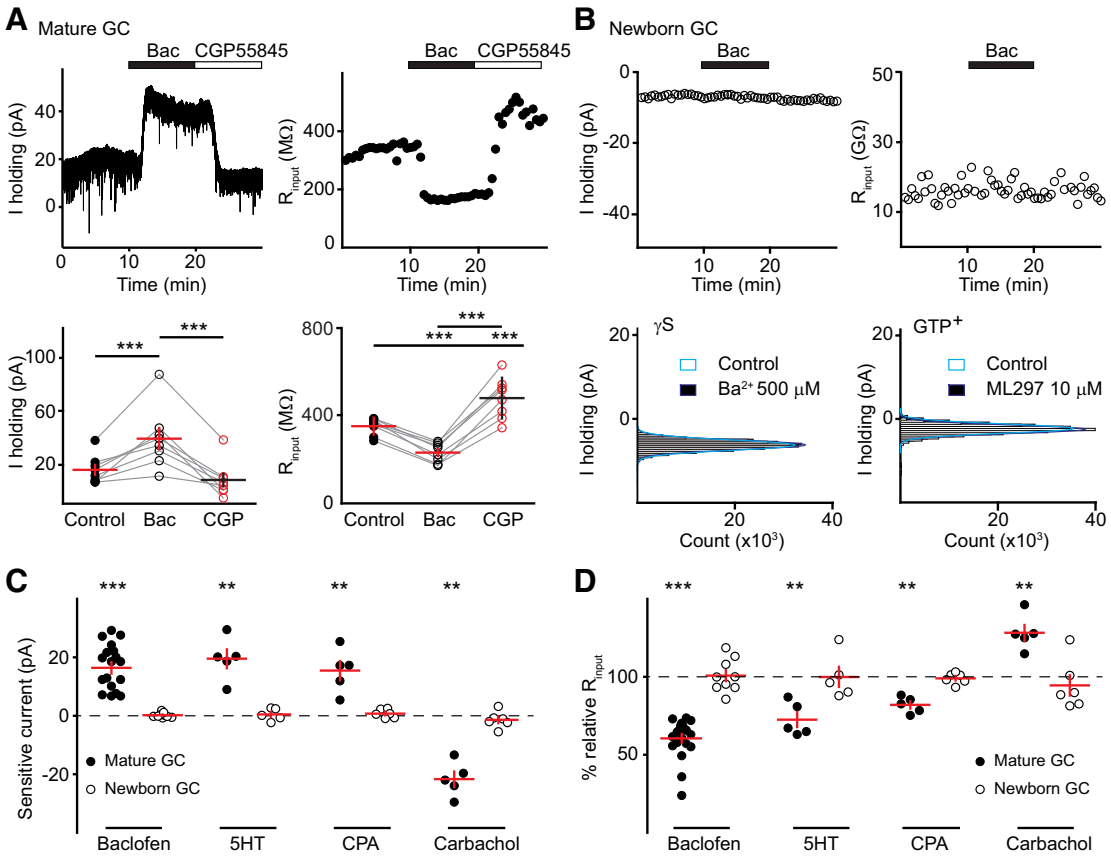

Figure 5. Newborn dentate GCs lack functional GIRK channels. ***A***, Top, Representative holding current from a mature GC held at −70 mV (left) and input resistance measured at 30 s intervals (right). Bottom, Baclofen (Bac; 30 μM; open black symbols) increased I_h values and reduced input resistance in a manner blocked by GCP55845 (CGP; 10 μM; open red symbols). Repeated-measures ANOVA: $F_{(2,14)} = 25.55$ and $F_{(2,14)} = 62.24$ for standing outward current and input resistance, respectively. Tukey's multiple-comparison *post hoc* test: ***$p < 0.001$; **$p < 0.01$. ***B***, Top, Representative holding current and input resistance from a newborn GC held at −70 mV, measured every 30 s. Bottom, all-points histograms made from 30 s segments show no effect of Ba^{2+} (500 μM, left) using an intracellular solution with γS or ML297 (10 μM, right) using GTP^+ internal. ***C***, ***D***, Summary of holding current and input resistance changes resulting from other metabotropic agonists coupled to GIRK channels in mature GCs (solid symbols) and newborn GCs (open symbols). Baclofen, 30 μM; 5-HT, 100 μM; CPA, 50 nM; and carbachol, 50 μM. Some experiments are performed at 22°C. Statistical one-sample *t* test differences from sample population against a theoretical mean value of 0 in ***C*** and 100 in ***D***. ***$p < 0.001$; **$p < 0.01$.

shown), confirming that newborn GCs lack constitutive activation of GIRK channels as well as activation by exogenous activators.

GIRK activation can be triggered by several neurotransmitters acting via $G_{i/o}$ proteins. To address whether newborn GCs specifically lack $GABA_B$ receptor-mediated GIRK coupling, we tested additional agonists of $G_{i/o}$ G protein-coupled receptors (GPCRs) including 5-hydroxytriptamine (5-HT; 10 μM) to target 5-HT_{1A} receptors (Andrade and Nicoll, 1987; Colino and Halliwell, 1987) and cyclopiazonic acid (CPA; 50 nM) to target A1 receptors (Trussell and Jackson, 1987; Thompson et al., 1992). Both agonists elicited a standing outward current with the consequent decrease of input resistance in mature GCs, and yet both failed to alter the membrane current or input resistance of newborn GCs (Fig. 5*C*,*D*). We further sought to inactivate GIRK currents via G_q proteins coupled to muscarinic receptors (Hill and Peralta, 2001; Lei et al., 2001). Carbachol (50 μM), a muscarinic receptor agonist that inhibits $GABA_B$-activated K^+ currents in hippocampal CA1 neurons (Sohn et al., 2007), induced a negative shift in the outward current and an increase in the input resistance of mature GCs. However, carbachol also had no effect on newborn GCs (Fig. 5*C*,*D*). Together, these results indicate that newborn GCs lack functional GIRK channels that contribute to the low intrinsic excitability of mature GCs.

Developmental profile of $GABA_B$-mediated GIRK activity in adult-born neurons

Since POMC-positive newborn GCs do not have functional GIRK channels, we wondered when the $GABA_B$/GIRK complex becomes functional during GC maturation. To address this question, we turned to synaptic activation to provide a robust measure of functional $GABA_B$/GIRK coupling in immature GCs that exhibit variable intrinsic properties related to their developmental stage. Since developing GCs at the same postmitotic age can exhibit a 10-fold range of input resistance (Heigele et al., 2016), it is difficult to make comparisons across newly generated cells using different intracellular solutions. We thus used electrical stimulation of the dentate medial molecular layer (MML) to recruit GABA release from local interneurons to generate a slow outward $GABA_B$-mediated GIRK current (Otis and Mody, 1992; Otis et al., 1993). Experiments were performed in slices from transgenic mice that enable the identification of adult-born neurons, including POMC-eGFP mice, GAD67-GFP mice to target GCs between ~1 and 3 weeks postmitosis (Zhao et al., 2010) and nestin-CreER^{TM4}/Ai14 mice to identify GCs at 3–5 weeks after tamoxifen induction. Recordings from unlabeled mature GCs in all mouse lines were interleaved with recordings from adult-born GCs.

In mature GCs (Fig. 6*A*, left), a single stimulus (200 μA, 100 μs) elicited a fast glutamatergic inward current and a biphasic

$GABA_A/GABA_B$ outward current. After blocking glutamate receptors (R-CPP, 10 μM; NBQX, 10 μM) and $GABA_A$ receptors [picrotoxin, 100 μM; gabazine (GBZ), 10 μM], the slow outward current peaked at ~250 ms following the stimulus (Fig. 6*A*, middle). This current was enhanced by the GABA transporter 1 (GAT1) inhibitor NO711 (10 μM) and was completely blocked by the inverse agonist CGP55845, consistent with a $GABA_B$-mediated K^+ current. Further confirming its identity, the synaptic $GABA_B$-mediated IPSC was absent in mature GCs from GIRK2 KO mice, even in the presence of NO711 (Fig. 6*A*, right, *D*). Synaptic $GABA_B$ responses were highly variable in immature GCs from Nestin and GAD67-GFP reporter mice, with some cells lacking $GABA_B$ IPSCs in both lines (Fig. 6*B*,*D*). Consistent with the lack of agonist-induced currents, all newborn GCs in POMC-GFP mice lacked synaptic $GABA_B$/GIRK responses despite the presence of NO711-sensitive (inward) $GABA_A$ receptor-mediated currents (Fig. 6*C*,*D*). To test whether synaptic $GABA_B$/GIRK responses correlated with constitutive GIRK signaling, we compared the effect of the inverse agonist CGP55845 on the input resistance of immature GCs with and without synaptic responses. Indeed, immature GCs with synaptic $GABA_B$/GIRK currents (Fig. 6*D*, right, solid symbols) exhibited an increase in input resistance following blockade of constitutive signaling with CGP55845, whereas immature GCs lacking synaptic currents showed no change in IR (Fig. 6*D*, right, open symbols; paired *t* test, $p = 0.0001$ and $p = 0.49$ for positive $GABA_B$ response and negative, respectively). Thus, the maturation of functional constitutive and synaptic $GABA_B$/GIRK signaling occurs in parallel.

Although the presence of synaptic and constitutive GIRK signaling in immature GCs was not strictly related to the reporter line, the majority of immature GCs with functional GIRK signaling were from Nestin-tdT mice (recorded at >3 weeks post-tamoxifen induction; Fig. 6*D*, right, red symbols) rather than GAD67-GFP mice (Fig. 6*D*, right, green symbols). This suggests that functional GIRK signaling develops after ~3 weeks of maturation, based on the timing of these reporter lines. But since the synaptic and constitutive current did not fully correlate with marker expression and the rate of new GC maturation is heterogeneous, we also tracked the development of $GABA_B$-GIRK activity using the input resistance as an independent measure of functional

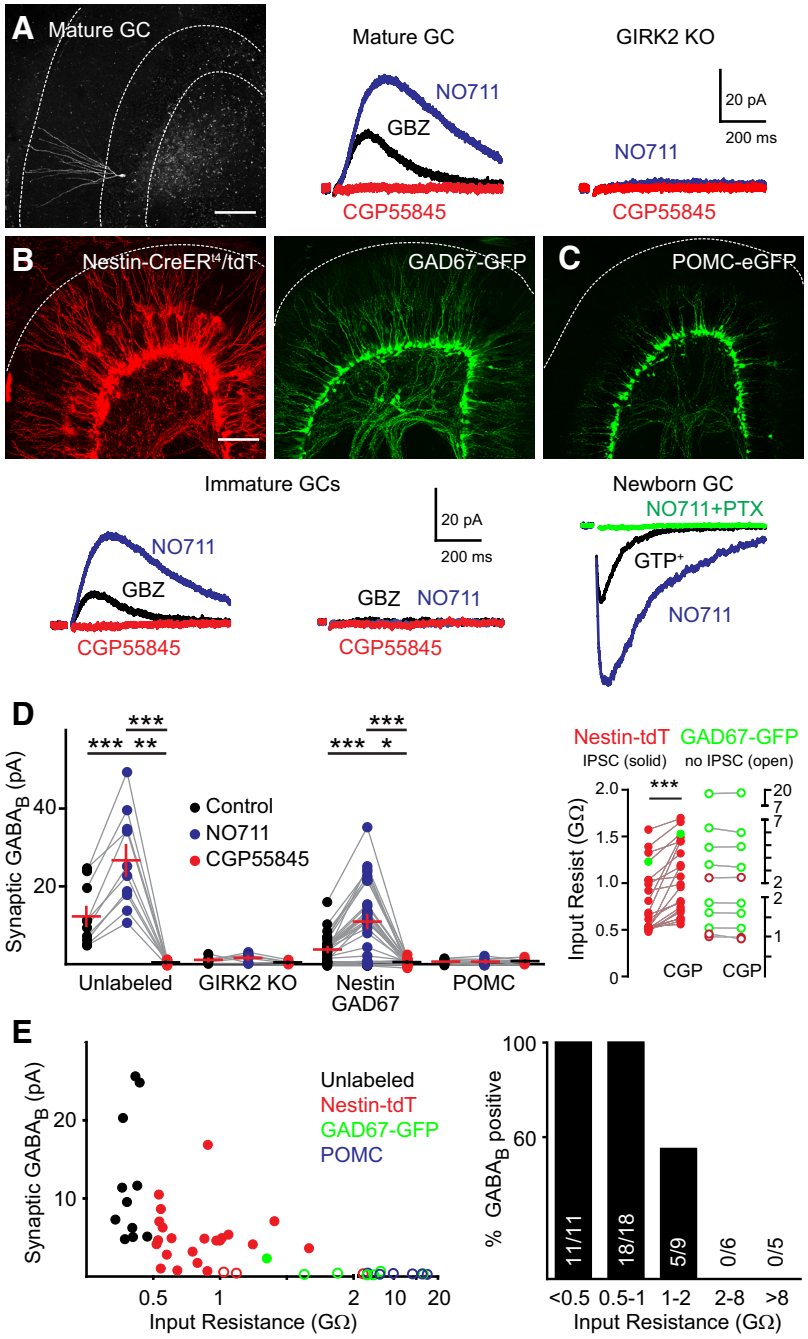

Figure 6. Development of $GABA_B$-mediated GIRK activity in adult-born GCs. ***A***, Left, Confocal image of a mature GC filled with biocytin. Scale bar, 100 μm. Middle, Stimulation in the middle molecular layer (100 μs; 200 μA) evokes a slow outward IPSC in mature GCs that is enhanced by the GAT1 blocker NO711 (5 μM, blue) and blocked by CGP55845 (10 μM, red). Each trace is an average of five sweeps. $GABA_A$ and glutamate receptors are blocked with gabazine (10 μM), R-CPP (10 μM), and NBQX (10 μM). Right, $GABA_B$-mediated slow IPSCs were absent in GIRK2 KO mice. ***B***, Top, Confocal images showing adult-born neurons in Nestin-CreER^{TM4}/tdTomato mice at 4 weeks after tamoxifen induction, and GAD67-GFP reporter mice. Bottom, Slow $GABA_B$-mediated IPSCs were recorded in immature GCs from Nestin-tdT and GAD67-GFP immature GCs, ***c***, but not in POMC-eGFP newborn GCs (despite $GABA_A$ receptor-mediated inward PSCs). ***D***, Left, Summary of $GABA_B$ IPSCs in unlabeled mature GCs (WT, $n = 10$), mature GCs from GIRK2 KO mice ($n = 7$), and immature GCs from Nestin-CreER and GAD67-GFP mice ($n = 32$) and newborn POMC-eGFP GCs ($n = 9$). The IPSC amplitude in control (black), NO711 (blue), and CGP55845 (red) are shown for each cell. Repeated-measures ANOVA: unlabeled (mature), $F_{(2,18)} = 41.43$; GIRK2 KO, $F_{(2,10)} = 2.95$; Nestin/GAD67, $F_{(2,62)} = 62.24$; POMC, $F_{(2,14)} = 0.27$. Tukey's multiple-comparison *post hoc* test: ***$p < 0.001$; **$p < 0.01$; *$p < 0.05$. Right, The effect of the $GABA_B$ inverse agonist CGP55845 on input resistance of immature GCs. Nestin-tdT immature GCs (red, $n = 24$), and GAD67-GFP immature GCs (green, $n = 9$) are separated by the presence (solid symbols) or absence (open symbols) of a synaptic $GABA_B$ IPSC, showing that only immature GCs with a synaptic $GABA_B$ IPSC exhibit constitutive $GABA_B$/GIRK signaling. Paired *t* test: $p = 0.0001$ and $p = 0.49$, respectively. ***E***, Slow IPSCs are present only in GCs with input resistance <2 GΩ. Solid symbols represent cells with $GABA_B$ IPSCs, and open symbols represent cells lacking a $GABA_B$ IPSC (even in NO711). Unlabeled mature GCs (black), Nestin-tdT (red), GAD67-GFP (green), and POMC-eGFP (blue) GCs. Right, Summary of the percentage of GCs with $GABA_B$ IPSCs (percentage $GABA_B$ positive).

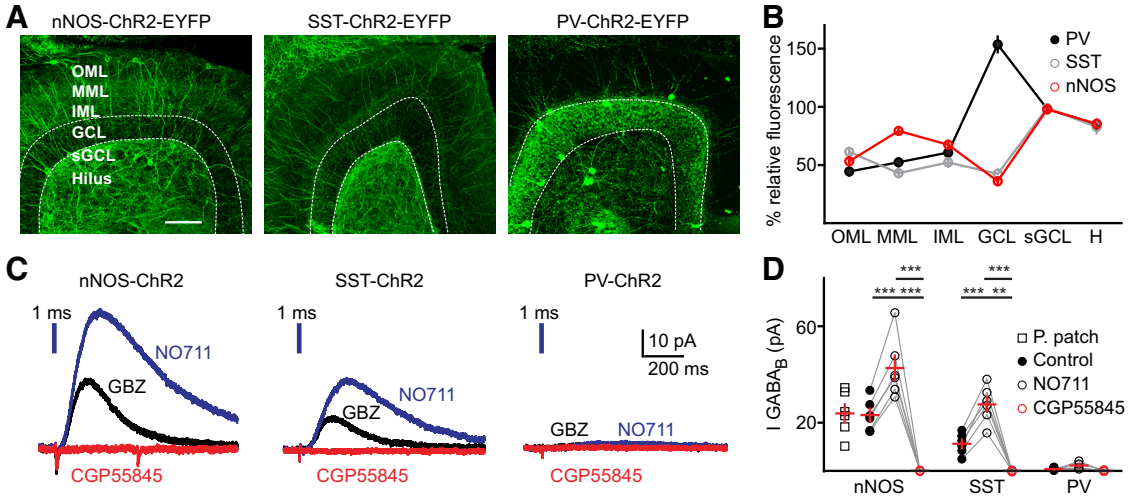

Figure 7. Dendritic GABA as source of $GABA_B$-evoked GIRK currents. ***A***, Confocal images of ChR2-EYFP expression in nNOS- (left), SST- (middle), and PV- (right) expressing interneurons. Scale bar, 100 μm. ***B***, Relative fluorescence measured in each GC layer from maximum *z*-projections (20 μm, 20 images) from each mouse line (nNOS, $n = 19$ sections; SST, $n = 6$ sections; PV, $n = 13$ sections). Fluorescence was normalized to the maximum signal in the sGCL. ***C***, Light-induced slow IPSCs in mature GCs from each ChR2-expressing line shown above, using 1 ms blue light pulses at maximum intensity. In the presence of gabazine (black), slow IPSCs were enhanced by NO711 (5 μM, blue) and blocked by CGP55845 (10 μM, red). Each trace is the average of five sweeps. ***D***, Summary of $GABA_B$ IPSC amplitudes in each condition. nNOS-ChR2, $n = 6$; SST-ChR2, $n = 6$; PV-ChR2, $n = 4$. Open squares show perforated patch recordings in nNOS-ChR2 mice ($n = 7$). Repeated-measures ANOVA: nNOS, $F_{(2,10)} = 66.23$; SST, $F_{(2,10)} = 69.56$; PV, $F_{(2,6)} = 4.92$. Tukey's multiple-comparison *post hoc* test: $^{***}p < 0.001$; $^{**}p < 0.01$; $^{*}p < 0.05$. There was no difference in the amplitude of IPSCs between perforated patch and whole-cell recordings; unpaired *t* test, $p = 0.87$. IML, Inner molecular layer; GCL, granular cell layer; sGCL, subgranular cell layer.

maturation (Fig. 6*E*). This analysis showed that the synaptic GIRK current first appears in developing GCs with an input resistance between 1 and 2 GΩ, a functional stage achieved, on average, ~3 weeks after mitosis (Mongiat et al., 2009; Dieni et al., 2013b; Heigele et al., 2016). All GCs with input resistance of >2 GΩ, including POMC-labeled GCs, did not exhibit synaptic $GABA_B$ responses or constitutive GIRK activity. Since $GABA_B$ receptors appear to be functional in proliferating progenitors (Giachino et al., 2014; see also Discussion), the lack of synaptic GIRK currents likely results from a lack of functional GIRK channels rather than $GABA_B$ receptors.

Interneuron subtype-selective synaptic $GABA_B$/GIRK activation

A diverse population of dentate interneurons provides GABA-mediated inhibition that is critical for maintaining sparse GCs integration of spatial and sensory information from entorhinal cortex. Dentate interneuron populations are typically classified by anatomical criteria, with distinct somatic or dendritic axonal projection patterns (Freund and Buzsáki, 1996). Since both $GABA_B$ receptors and GIRK channels exhibit a laminar distribution pattern in dentate and other cerebral areas (Fritschy et al., 1999; Kulik et al., 2006; Degro et al., 2015), we wondered whether specific interneuron subtypes would be the source of synaptic $GABA_B$/GIRK signaling to GCs. Using transgenic mice expressing ChR2 in biochemically defined interneuron populations, we compared $GABA_B$-mediated synaptic currents evoked by selective activation of nNOS-, SST-, and PV-expressing interneurons. As shown in Figure 7*A*, nNOS- and SST-expressing interneurons project to the molecular layer, providing dendritic inhibition. In contrast, PV interneurons target the granule cell layer, providing somatic inhibition to GCs (Hu et al., 2014). These expected projection patterns were semiquantified by measuring the relative fluorescence of CHR2-EYFP in each layer (Fig. 7*B*). Although all interneuron subtypes had dense processes in the hilus and PVs clearly targeted the granule cell layer, nNOS and SST interneurons showed complementary dendritic projecting patterns with dense nNOS-EYFP processes in the MML and dense SST-EYFP process in the outer molecular layer (OML).

In recordings from mature GCs, optogenetic stimulation of each interneuron subtype (455 nm, 1 ms, maximum intensity) generated large $GABA_A$ receptor-mediated IPSCs with similar amplitudes (nNOS interneurons, 1.12 ± 0.08 nA; SST interneurons, 0.93 ± 0.12 nA; PV interneurons, 1.33 ± 0.11 nA; Cl^--based internal solution), confirming robust GABA release following optogenetic stimulation. In the presence of GBZ (10 μM), single blue light stimuli of nNOS interneurons generated a slow outward current that, like with electric stimulation, was enhanced by NO711 and blocked by CGP55845 (Fig. 7*C*,*D*, left). Optogenetic stimulation of SST interneurons under the same conditions generated a measurable but smaller GIRK current that was enhanced by NO711 and blocked by CGP55845 (Fig. 7*C*,*D*, middle). However, optogenetic stimulation of PV interneurons with single stimuli failed to evoke measurable currents, even in NO711 (Fig. 7*C*,*D*, right). Furthermore, when we performed perforated patch recordings from GCs to maintain native intracellular milieu, the amplitude and kinetic profile of $GABA_B$-mediated currents evoked by optogenetic stimulation of nNOS interneurons were indistinguishable from currents recorded in whole-cell configuration (Fig. 7*D*, open symbols). Altogether, these data indicate that nNOS-expressing neurogliaform interneurons are the primary source of $GABA_B$ receptor-mediated slow inhibition in DG, as described in other brain regions (Tamás et al., 2003; Armstrong et al., 2011; Overstreet-Wadiche and McBain, 2015).

Discussion

Here we demonstrate that GIRK channels influence mature GC excitability via two mechanisms. First, constitutive GIRK activity affects RMP and input resistance, contributing to the hallmark low intrinsic excitability of GCs. This tonic form of channel activity is regulated by G protein $\beta\gamma$ subunit availability, which is under the control of the GTP/GDP system. Second, synaptic GABA release by dendritic-targeting interneurons that express SST or nNOS evokes phasic activation of $GABA_B$-mediated GIRK

channel activity that likely plays a role in the dynamic integration of ongoing synaptic activity. Interestingly, adult-generated GCs initially lack both constitutive and synaptic GABAB/GIRK channel activity that develops over 3–4 weeks to provide more mature integrative properties. Together, these results provide a comprehensive characterization of the physiological function, maturation, and sources of postsynaptic $GABA_B$/GIRK inhibition in dentate GCs that suggest this signaling pathway contributes to sparse activity patterns *in vivo*.

GIRK constitutive activity contributes to low excitability of dentate GCs

The low intrinsic excitability of GCs in combination with strong inhibitory GABAergic circuitry are often recognized as central components in sparse DG activity. Yet, as mentioned, reports of RMP and input resistance from whole-cell recordings of GCs vary widely, and one source of variability may stem from whether GTP was included in the intracellular solution. Although millimolar concentrations of intracellular GTP generate a hyperpolarized RMP in CA1 pyramidal cells via constitutive GIRK activity (Lüscher et al., 1997), we did not detect this effect with submillimolar concentrations. Our data therefore suggest a unique mechanism in dentate GCs wherein submillimolar intracellular GTP is sufficient for constitutive GIRK activity. Indeed, we found that genetic deletion of GIRK2 channels and pharmacological manipulations of those channels or the GTP system dramatically changes excitability in mature GCs.

What can generate constitutive GIRK channel activity? GIRK channels are tetramers with four pockets to bind $\beta\gamma$ subunits (Corey and Clapham, 2001). Occupancy of some of those pockets is sufficient to generate receptor-independent basal GIRK channel activity that probably depends on free $\beta\gamma$ subunits availability, which can be regulated by other components of the $GABA_B$/GIRK complex (Ivanova-Nikolova et al., 1998). For example, RGS proteins (regulators of G protein signaling) interact directly with Gα subunits to enhance GTPase activity (Doupnik, 2015). Different density-, region-, or compartment-specific expression of RGS proteins could therefore contribute to differences in constitutive GIRK activation by similar levels of exogenous GTP in pyramidal cells and GCs (Gold et al., 1997; Lüscher et al., 1997; Drenan et al., 2006; Morgans et al., 2007). We found that reducing $\beta\gamma$ subunit availability (βS or GTP^-), blocking GIRK channels (Ba^{2+}, tertiapin-Q), or genetically deleting GIRK channels (GIRK2 KO) increased GC excitability, whereas pharmacological GIRK activation (ML297) or raising $\beta\gamma$ availability (γS) reduced excitability beyond GTP alone. This suggests an intermediate level of basal GIRK activation that can be modulated under physiological conditions to adjust excitability, as occurs in other brain regions (Lüscher et al., 1997; Torrecilla et al., 2002; Wiser et al., 2006) or in the heart (Voigt et al., 2014).

Of course, many GPCRs are poised to modulate GTP-dependent basal GIRK activity. Low levels of ambient GABA have been implicated in persistent activation of $GABA_A$ receptors on GCs (Overstreet and Westbrook, 2001; Nusser and Mody, 2002; Wei et al., 2004; Mtchedlishvili and Kapur, 2006). However, we found the $GABA_B$ receptor competitive antagonist CGP35348 had only a minor effect on input resistance and did not significantly alter RMP or GC spiking properties in response to somatic current injection. In contrast, the $GABA_B$ inverse agonist CGP55845 (Mukherjee et al., 2006) more strongly affected IR, RMP, and rheobase. Together, this supports the existence of precoupled $GABA_B$/G protein/GIRK complex with constitutive activity that is independent of ligand binding, as suggested for other GPCRs that respond to dopamine or opioids (Luján et al., 2014; Nagi and Pineyro, 2014). Pilot experiments showed that competitive antagonists for other $G_{i/o}$-coupled receptors had minimal or no effects on RMP and input resistance (data not shown), although we cannot rule out a contribution of constitutive GIRK activation arising from concerted effects of many converging metabotropic receptors. Yet, constitutive ligand-independent activity of GIRK channels is a common feature in heterologous systems, suggesting that it is also present in intact systems (Doupnik et al., 1997; Saitoh et al., 1997; Zhang et al., 2002; Xie et al., 2010).

GIRK channels contribute to mature excitability during neurogenesis

Newborn GCs have high excitability due to an input resistance that is much higher than that of mature GCs (Overstreet et al., 2004; Schmidt-Hieber et al., 2004) and that of an RMP that is slightly more depolarized ($\sim$ 10 mV; (Heigele et al., 2016). One characteristic of mature GCs that is absent in developing GCs <3 weeks of age is the ability to fire repetitive spike trains, a function that is provided by high K_{ir} channel expression (Mongiat et al., 2009). Our data suggest that delayed expression of GIRK channels also contributes to the high IR and depolarized RMP of immature GCs. It will be important to include constitutively active GIRKs with models of mature and developing GCs, since the differing biophysical properties of GIRKs and K_{ir} channels will undoubtedly confer distinct physiological consequences (Beining et al., 2017). Other classes of ion channels also change expression levels or properties during GC maturation. For example, the small amplitude and depolarized threshold for action potentials in very young GCs likely results from a low density of voltage-gated Na^+ channels (Overstreet et al., 2004; Espósito et al., 2005; Mongiat et al., 2009; Dieni et al., 2013b), and we have not observed the hyperpolarization-induced sag that reflects I_h (J. Gonzalez, L. Overstreet-Wadiche unpublished observations). Likewise, young GCs display prominent T-type Ca^{2+} spikes, high NMDAR2B receptor content and NKCC1 transporters that differentiate them from mature GCs (Schmidt-Hieber et al., 2004; Ge et al., 2006, 2007; Chancey et al., 2013). In addition to the biological significance of these differences, the lack of GIRK channel activity in young GCs may preclude chemogenic suppression of activity using engineered GPCRs that couple to endogenous GIRK channels.

Despite the lack of functional GIRK-mediated inhibition at early stages, $GABA_B$-mediated signaling may be important in the neurogenic process. Conditional deletion of $GABA_B$ receptors in Nestin-expressing stem cells enhances proliferation, suggesting that functional $GABA_B$ receptors suppress stem cell activity (Giachino et al., 2014). Other neurodevelopmental functions of $GABA_B$ signaling have also been described (Gaiarsa and Porcher, 2013), pointing to the early expression of functional $GABA_B$ receptors with subsequent expression of GIRKs enabling inhibition mediated by the $GABA_B$/GIRK complex. Indeed, viral-mediated expression of GIRK in embryonic hippocampal neurons is sufficient to generate $GABA_B$-mediated GIRK activation by endogenous $GABA_B$ receptors (Ehrengruber et al., 1997). Thus, functional GIRK channel expression may convert $GABA_B$ receptor signaling from a trophic to an inhibitory function in a manner analogous to the role of the Cl^- exporter KCC2 in the developmental switch of $GABA_A$ receptor signaling.

As low excitability develops during GC maturation, new GCs also become integrated into the hippocampal circuit. The inverse relationship between intrinsic excitability and synaptic integra-

tion suggests that the high excitability of immature GCs is counteracted by low excitatory innervation (Dieni et al., 2013b, 2016; Li et al., 2017). Late expression of functional GIRK channels further suggests the possibility that the formation of excitatory synaptic connectivity contributes to the maturation of functional $GABA_B$/GIRK complexes. Interestingly, at the early developmental stage when adult-born GCs entirely lack GIRK channels they also lack functional AMPA receptor-containing synapses (Chancey et al., 2013). In addition to the developmental regulation of alternative variants of $GABA_B$R subunits (Fritschy et al., 1999), the expression level and trafficking of GIRK channels in the hippocampus increases during postnatal development to reach adult levels during the period of excitatory synaptogenesis (López-Bendito et al., 2004; Fernández-Alacid et al., 2011). The absence of functional GIRKs in newborn GCs along with the maturation of the functional $GABA_B$/GIRK complex around the third week postmitosis supports the idea that constitutive and synaptic $GABA_B$-mediated inhibition develops in parallel with the maturation of excitatory synapses.

Neurogliaform interneurons are a primary source of slow phasic inhibition

Immunohistochemical and *in situ* hybridization studies have shown that GIRK subunits are mainly expressed in somatodendritic domains (Kulik et al., 2006; Saenz del Burgo et al., 2008; Fernández-Alacid et al., 2011). Similarly, $GABA_B$Rs colocalize with GIRK channels predominantly in dendritic regions (Kulik et al., 2006; Degro et al., 2015). This laminar distribution of $GABA_B$R and GIRK channels coincides with a marked polarity in the axonal distribution of the different interneuron populations in the DG. Parvalbumin-expressing interneurons are primarily fast-spiking basket cells that target axons to the granular layer (Freund and Buzsáki, 1996; Hu et al., 2014). The fact that large $GABA_A$ currents evoked by PV-ChR2 are not accompanied by measurable GIRK currents is consistent with the anatomical distribution of GIRK channels in the distal dendrites of different cell types and brain regions (Degro et al., 2015). In contrast, both dendritic projecting SST and nNOS interneurons generated phasic $GABA_B$/GIRK currents, with the larger currents evoked by nNOS cells (despite $GABA_A$ currents of similar amplitude) likely reflects their differing mode of transmission. nNOS-expressing interneurons are largely made up of Ivy/neurogliaform interneurons (Overstreet-Wadiche and McBain, 2015), which use a form of volume transmission that reaches both synaptic and nonsynaptic GABA receptors located relatively far from release sites (Oláh et al., 2009). We predict that $GABA_B$/GIRK inhibition provided by nNOS interneurons plays an important role in the regulation of dendritic integration of cortical input, and that both constitutive and phasic GIRK-mediated inhibition strongly contribute to sparse DG activity as well as the distinct information-processing capabilities of developing and mature GCs. Dysregulation of this signaling cascade could also contribute to serious pathologies such as epilepsy.

References

Andrade R, Nicoll RA (1987) Pharmacologically distinct actions of serotonin on single pyramidal neurones of the rat hippocampus recorded in vitro. J Physiol 394:99–124. CrossRef Medline

Andrade R, Malenka RC, Nicoll RA (1986) A G protein couples serotonin and GABAB receptors to the same channels in hippocampus. Science 234:1261–1265. CrossRef Medline

Armstrong C, Szabadics J, Tamás G, Soltesz I (2011) Neurogliaform cells in the molecular layer of the dentate gyrus as feed-forward gamma-aminobutyric acidergic modulators of entorhinal-hippocampal interplay. J Comp Neurol 519:1476–1491. CrossRef Medline

Beck H, Ficker E, Heinemann U (1992) Properties of two voltage-activated potassium currents in acutely isolated juvenile rat dentate gyrus granule cells. J Neurophysiol 68:2086–2099. CrossRef Medline

Beck H, Clusmann H, Kral T, Schramm J, Heinemann U, Elger CE (1997) Potassium currents in acutely isolated human hippocampal dentate granule cells. J Physiol 498:73–85. CrossRef Medline

Beining M, Mongiat LA, Schwarzacher SW, Cuntz H, Jedlicka P (2017) T2N as a new tool for robust electrophysiological modeling demonstrated for mature and adult-born dentate granule cells. Elife 6:e26517. CrossRef Medline

Breitwieser GE, Szabo G (1988) Mechanism of muscarinic receptor-induced K+ channel activation as revealed by hydrolysis-resistant GTP analogues. J Gen Physiol 91:469–493. CrossRef Medline

Brucato FH, Mott DD, Lewis DV, Swartzwelder HS (1995) GABAB receptors modulate synaptically-evoked responses in the rat dentate gyrus, in vivo. Brain Res 677:326–332. CrossRef Medline

Brunner J, Ster J, Van-Weert S, Andrási T, Neubrandt M, Corti C, Corsi M, Ferraguti F, Gerber U, Szabadics J (2013) Selective silencing of individual dendritic branches by an mGlu2-activated potassium conductance in dentate gyrus granule cells. J Neurosci 33:7285–7298. CrossRef Medline

Brunner J, Neubrandt M, Van-Weert S, Andrási T, Kleine Borgmann FB, Jessberger S, Szabadics J (2014) Adult-born granule cells mature through two functionally distinct states. Elife 3:e03104. CrossRef Medline

Canning KJ, Leung LS (2000) Excitability of rat dentate gyrus granule cells in vivo is controlled by tonic and evoked GABA(B) receptor-mediated inhibition. Brain Res 863:271–275. CrossRef Medline

Chancey JH, Adlaf EW, Sapp MC, Pugh PC, Wadiche JI, Overstreet-Wadiche LS (2013) GABA depolarization is required for experience-dependent synapse unsilencing in adult-born neurons. J Neurosci 33:6614–6622. CrossRef Medline

Chawla MK, Guzowski JF, Ramirez-Amaya V, Lipa P, Hoffman KL, Marriott LK, Worley PF, McNaughton BL, Barnes CA (2005) Sparse, environmentally selective expression of arc RNA in the upper blade of the rodent fascia dentata by brief spatial experience. Hippocampus 15:579–586. CrossRef Medline

Chen X, Johnston D (2005) Constitutively active G protein-gated inwardly rectifying K^+ channels in dendrites of hippocampal CA1 pyramidal neurons. J Neurosci 25:3787–3792. CrossRef Medline

Chiang PH, Wu PY, Kuo TW, Liu YC, Chan CF, Chien TC, Cheng JK, Huang YY, Chiu CD, Lien CC (2012) GABA is depolarizing in hippocampal dentate granule cells of the adolescent and adult rats. J Neurosci 32:62–67. CrossRef Medline

Colino A, Halliwell JV (1987) Differential modulation of three separate K-conductances in hippocampal CA1 neurons by serotonin. Nature 328:73–77. CrossRef Medline

Corey S, Clapham DE (2001) The stoichiometry of gbeta gamma binding to G protein-regulated inwardly rectifying K+ channels (GIRKs). J Biol Chem 276:11409–11413. CrossRef Medline

Coulter DA, Carlson GC (2007) Functional regulation of the dentate gyrus by GABA-mediated inhibition. Prog Brain Res 163:235–243. CrossRef Medline

Cowley MA, Smart JL, Rubinstein M, Cerdán MG, Diano S, Horvath TL, Cone RD, Low MJ (2001) Leptin activates anorexigenic POMC neurons through a neural network in the arcuate nucleus. Nature 411:480–484. CrossRef Medline

Degro CE, Kulik A, Booker SA, Vida I (2015) Compartmental distribution of GABAB receptor-mediated currents along the somatodendritic axis of hippocampal principal cells. Front Synaptic Neurosci 7:6. CrossRef Medline

De Koninck Y, Mody I (1997) Endogenous GABA activates small-conductance K+ channels underlying slow IPSCs in rat hippocampal neurons. J Neurophysiol 77:2202–2208. CrossRef Medline

Dieni CV, Chancey JH, Overstreet-Wadiche LS (2013a) Dynamic functions of GABA signaling during granule cell maturation. Front Neural Circuits 6:113. CrossRef Medline

Dieni CV, Nietz AK, Panichi R, Wadiche JI, Overstreet-Wadiche L (2013b) Distinct determinants of sparse activation during granule cell maturation. J Neurosci 33:19131–19142. CrossRef Medline

Dieni CV, Panichi R, Aimone JB, Kuo CT, Wadiche JI, Overstreet-Wadiche L

(2016) Low excitatory innervation balances high intrinsic excitability of immature dentate neurons. Nat Commun 7:11313. CrossRef Medline

Doupnik CA (2015) RGS redundancy and implications in GPCR-GIRK signaling. Int Rev Neurobiol 123:87–116. CrossRef Medline

Doupnik CA, Davidson N, Lester HA, Kofuji P (1997) RGS proteins reconstitute the rapid gating kinetics of gbetagamma-activated inwardly rectifying K+ channels. Proc Natl Acad Sci U S A 94:10461–10466. CrossRef Medline

Drenan RM, Doupnik CA, Jayaraman M, Buchwalter AL, Kaltenbronn KM, Huettner JE, Linder ME, Blumer KJ (2006) R7BP augments the function of RGS7*Gbeta5 complexes by a plasma membrane-targeting mechanism. J Biol Chem 281:28222–28231. CrossRef Medline

Dutar P, Nicoll RA (1988) A physiological role for GABAB receptors in the central nervous system. Nature 332:156–158. CrossRef Medline

Ehrengruber MU, Doupnik CA, Xu Y, Garvey J, Jasek MC, Lester HA, Davidson N (1997) Activation of heteromeric G protein-gated inward rectifier K+ channels overexpressed by adenovirus gene transfer inhibits the excitability of hippocampal neurons. Proc Natl Acad Sci U S A 94:7070–7075. CrossRef Medline

Espósito MS, Piatti VC, Laplagne DA, Morgenstern NA, Ferrari CC, Pitossi FJ, Schinder AF (2005) Neuronal differentiation in the adult hippocampus recapitulates embryonic development. J Neurosci 25:10074–10086. CrossRef Medline

Ewell LA, Jones MV (2010) Frequency-tuned distribution of inhibition in the dentate gyrus. J Neurosci 30:12597–12607. CrossRef Medline

Fernández-Alacid L, Watanabe M, Molnár E, Wickman K, Luján R (2011) Developmental regulation of G protein-gated inwardly-rectifying K+ (GIRK/Kir3) channel subunits in the brain. Eur J Neurosci 34:1724–1736. CrossRef Medline

Foster JD, Kitchen I, Bettler B, Chen Y (2013) GABAB receptor subtypes differentially modulate synaptic inhibition in the dentate gyrus to enhance granule cell output. Br J Pharmacol 168:1808–1819. CrossRef Medline

French RJ, Shoukimas JJ (1985) An ion's view of the potassium channel. the structure of the permeation pathway as sensed by a variety of blocking ions. J Gen Physiol 85:669–698. CrossRef Medline

Freund TF, Buzsáki G (1996) Interneurons of the hippocampus. Hippocampus 6:347–470. CrossRef Medline

Fritschy JM, Meskenaite V, Weinmann O, Honer M, Benke D, Mohler H (1999) GABAB-receptor splice variants GB1a and GB1b in rat brain: developmental regulation, cellular distribution and extrasynaptic localization. Eur J Neurosci 11:761–768. CrossRef Medline

Gaiarsa JL, Porcher C (2013) Emerging neurotrophic role of GABAB receptors in neuronal circuit development. Front Cell Neurosci 7:206. CrossRef Medline

Ge S, Goh EL, Sailor KA, Kitabatake Y, Ming GL, Song H (2006) GABA regulates synaptic integration of newly generated neurons in the adult brain. Nature 439:589–593. CrossRef Medline

Ge S, Pradhan DA, Ming GL, Song H (2007) GABA sets the tempo for activity-dependent adult neurogenesis. Trends Neurosci 30:1–8. CrossRef Medline

Giachino C, Barz M, Tchorz JS, Tome M, Gassmann M, Bischofberger J, Bettler B, Taylor V (2014) GABA suppresses neurogenesis in the adult hippocampus through GABAB receptors. Development 141:83–90. CrossRef Medline

Gold SJ, Ni YG, Dohlman HG, Nestler EJ (1997) Regulators of G protein signaling (RGS) proteins: region-specific expression of nine subtypes in rat brain. J Neurosci 17:8024–8037. CrossRef Medline

Harnett MT, Xu NL, Magee JC, Williams SR (2013) Potassium channels control the interaction between active dendritic integration compartments in layer 5 cortical pyramidal neurons. Neuron 79:516–529. CrossRef Medline

Heigele S, Sultan S, Toni N, Bischofberger J (2016) Bidirectional GABAergic control of action potential firing in newborn hippocampal granule cells. Nat Neurosci 19:263–270. CrossRef Medline

Hernández-Rabaza V, Hontecillas-Prieto L, Velázquez-Sánchez C, Ferragud A, Pérez-Villaba A, Arcusa A, Barcia JA, Trejo JL, Canales JJ (2008) The hippocampal dentate gyrus is essential for generating contextual memories of fear and drug-induced reward. Neurobiol Learn Mem 90:553–559. CrossRef Medline

Hibino H, Inanobe A, Furutani K, Murakami S, Findlay I, Kurachi Y (2010) Inwardly rectifying potassium channels: their structure, function, and physiological roles. Physiol Rev 90:291–366. CrossRef Medline

Hill JJ, Peralta EG (2001) Inhibition of a gi-activated potassium channel (GIRK1/4) by the gq-coupled m1 muscarinic acetylcholine receptor. J Biol Chem 276:5505–5510. CrossRef Medline

Hsu D (2007) The dentate gyrus as a filter or gate: a look back and a look ahead. Prog Brain Res 163:601–613. CrossRef Medline

Hu H, Gan J, Jonas P (2014) Interneurons. Fast-spiking, parvalbumin(+) GABAergic interneurons: from cellular design to microcircuit function. Science 345:1255263. CrossRef Medline

Ivanova-Nikolova TT, Nikolov EN, Hansen C, Robishaw JD (1998) Muscarinic K+ channel in the heart. modal regulation by G protein beta gamma subunits. J Gen Physiol 112:199–210. CrossRef Medline

Jin W, Lu Z (1999) Synthesis of a stable form of tertiapin: a high-affinity inhibitor for inward-rectifier K+ channels. Biochemistry 38:14286–14293. CrossRef Medline

Jung MW, McNaughton BL (1993) Spatial selectivity of unit activity in the hippocampal granular layer. Hippocampus 3:165–182. CrossRef Medline

Kaufmann K, Romaine I, Days E, Pascual C, Malik A, Yang L, Zou B, Du Y, Sliwoski G, Morrison RD, Denton J, Niswender CM, Daniels JS, Sulikowski GA, Xie XS, Lindsley CW, Weaver CD (2013) ML297 (VU0456810), the first potent and selective activator of the GIRK potassium channel, displays antiepileptic properties in mice. ACS Chem Neurosci 4:1278–1286. CrossRef Medline

Kim CS, Johnston D (2015) A1 adenosine receptor-mediated GIRK channels contribute to the resting conductance of CA1 neurons in the dorsal hippocampus. J Neurophysiol 113:2511–2523. CrossRef Medline

Kirchheim F, Tinnes S, Haas CA, Stegen M, Wolfart J (2013) Regulation of action potential delays via voltage-gated potassium Kv1.1 channels in dentate granule cells during hippocampal epilepsy. Front Cell Neurosci 7:248. CrossRef Medline

Kowalski J, Gan J, Jonas P, Pernía-Andrade AJ (2016) Intrinsic membrane properties determine hippocampal differential firing pattern in vivo in anesthetized rats. Hippocampus 26:668–682. CrossRef Medline

Kulik A, Vida I, Fukazawa Y, Guetg N, Kasugai Y, Marker CL, Rigato F, Bettler B, Wickman K, Frotscher M, Shigemoto R (2006) Compartment-dependent colocalization of Kir3.2-containing K^+ channels and $GABA_B$ receptors in hippocampal pyramidal cells. J Neurosci 26:4289–4297. CrossRef Medline

Kuo CT, Mirzadeh Z, Soriano-Navarro M, Rasin M, Wang D, Shen J, Sestan N, Garcia-Verdugo J, Alvarez-Buylla A, Jan LY, Jan YN (2006) Postnatal deletion of Numb/Numblike reveals repair and remodeling capacity in the subventricular neurogenic niche. Cell 127:1253–1264. CrossRef Medline

Laplagne DA, Espósito MS, Piatti VC, Morgenstern N, Zhao C, van Praag H, Gage FH, Schinder AF (2006) Functional convergence of neurons generated in the developing and adult hippocampus. PLoS Biol 4:e409. CrossRef Medline

Lei Q, Talley EM, Bayliss DA (2001) Receptor-mediated inhibition of G protein-coupled inwardly rectifying potassium channels involves G(alpha)q family subunits, phospholipase C, and a readily diffusible messenger. J Biol Chem 276:16720–16730. CrossRef Medline

Leutgeb JK, Leutgeb S, Moser MB, Moser EI (2007) Pattern separation in the dentate gyrus and CA3 of the hippocampus. Science 315:961–966. CrossRef Medline

Li L, Sultan S, Heigele S, Schmidt-Salzmann C, Toni N, Bischofberger J (2017) Silent synapses generate sparse and orthogonal action potential firing in adult-born hippocampal granule cells. Elife 6:e23612. CrossRef Medline

Liu X, Ramirez S, Tonegawa S (2014) Inception of a false memory by optogenetic manipulation of a hippocampal memory engram. Philos Trans R Soc Lond B Biol Sci 369:20130142. CrossRef Medline

Liu YB, Lio PA, Pasternak JF, Trommer BL (1996) Developmental changes in membrane properties and postsynaptic currents of granule cells in rat dentate gyrus. J Neurophysiol 76:1074–1088. CrossRef Medline

López-Bendito G, Shigemoto R, Kulik A, Vida I, Fairén A, Luján R (2004) Distribution of metabotropic GABA receptor subunits GABAB1a/b and GABAB2 in the rat hippocampus during prenatal and postnatal development. Hippocampus 14:836–848. CrossRef Medline

Luján R, Marron Fernandez de Velasco E, Aguado C, Wickman K (2014) New insights into the therapeutic potential of girk channels. Trends Neurosci 37:20–29. CrossRef Medline

Lüscher C, Slesinger PA (2010) Emerging roles for G protein-gated inwardly rectifying potassium (GIRK) channels in health and disease. Nat Rev Neurosci 11:301–315. CrossRef Medline

Lüscher C, Jan LY, Stoffel M, Malenka RC, Nicoll RA (1997) G protein-coupled inwardly rectifying K+ channels (GIRKs) mediate postsynaptic but not presynaptic transmitter actions in hippocampal neurons. Neuron 19:687–695. CrossRef Medline

Mongiat LA, Espósito MS, Lombardi G, Schinder AF (2009) Reliable activation of immature neurons in the adult hippocampus. PLoS One 4:e5320. CrossRef Medline

Morgans CW, Weiwei L, Wensel TG, Brown RL, Perez-Leon JA, Bearnot B, Duvoisin RM (2007) Gbeta5-RGS complexes co-localize with mGluR6 in retinal ON-bipolar cells. Eur J Neurosci 26:2899–2905. CrossRef Medline

Mott DD, Lewis DV (1992) GABAB receptors mediate disinhibition and facilitate long-term potentiation in the dentate gyrus. Epilepsy Res Suppl 7:119–134. Medline

Mott DD, Xie CW, Wilson WA, Swartzwelder HS, Lewis DV (1993) GABAB autoreceptors mediate activity-dependent disinhibition and enhance signal transmission in the dentate gyrus. J Neurophysiol 69:674–691. CrossRef Medline

Mott DD, Li Q, Okazaki MM, Turner DA, Lewis DV (1999) GABAB-receptor-mediated currents in interneurons of the dentate-hilus border. J Neurophysiol 82:1438–1450. CrossRef Medline

Mtchedlishvili Z, Kapur J (2006) High-affinity, slowly desensitizing GABAA receptors mediate tonic inhibition in hippocampal dentate granule cells. Mol Pharmacol 69:564–575. CrossRef Medline

Mukherjee RS, McBride EW, Beinborn M, Dunlap K, Kopin AS (2006) Point mutations in either subunit of the GABAB receptor confer constitutive activity to the heterodimer. Mol Pharmacol 70:1406–1413. CrossRef Medline

Nagi K, Pineyro G (2014) Kir3 channel signaling complexes: focus on opioid receptor signaling. Front Cell Neurosci 8:186. CrossRef Medline

Neunuebel JP, Knierim JJ (2012) Spatial firing correlates of physiologically distinct cell types of the rat dentate gyrus. J Neurosci 32:3848–3858. CrossRef Medline

Nusser Z, Mody I (2002) Selective modulation of tonic and phasic inhibitions in dentate gyrus granule cells. J Neurophysiol 87:2624–2628. CrossRef Medline

Oláh S, Füle M, Komlósi G, Varga C, Báldi R, Barzó P, Tamás G (2009) Regulation of cortical microcircuits by unitary GABA-mediated volume transmission. Nature 461:1278–1281. CrossRef Medline

Otis TS, Mody I (1992) Differential activation of GABAA and GABAB receptors by spontaneously released transmitter. J Neurophysiol 67:227–235. CrossRef Medline

Otis TS, De Koninck Y, Mody I (1993) Characterization of synaptically elicited GABAB responses using patch-clamp recordings in rat hippocampal slices. J Physiol 463:391–407. CrossRef Medline

Overstreet LS, Westbrook GL (2001) Paradoxical reduction of synaptic inhibition by vigabatrin. J Neurophysiol 86:596–603. CrossRef Medline

Overstreet LS, Hentges ST, Bumaschny VF, de Souza FS, Smart JL, Santangelo AM, Low MJ, Westbrook GL, Rubinstein M (2004) A transgenic marker for newly born granule cells in dentate gyrus. J Neurosci 24:3251–3259. CrossRef Medline

Overstreet-Wadiche L, McBain CJ (2015) Neurogliaform cells in cortical circuits. Nat Rev Neurosci 16:458–468. CrossRef Medline

Overstreet-Wadiche LS, Westbrook GL (2006) Functional maturation of adult-generated granule cells. Hippocampus 16:208–215. CrossRef Medline

Pernía-Andrade AJ, Jonas P (2014) Theta-gamma-modulated synaptic currents in hippocampal granule cells in vivo define a mechanism for network oscillations. Neuron 81:140–152. CrossRef Medline

Pinard A, Seddik R, Bettler B (2010) GABAB receptors: physiological functions and mechanisms of diversity. Adv Pharmacol 58:231–255. CrossRef Medline

Price CJ, Scott R, Rusakov DA, Capogna M (2008) $GABA_B$ receptor modulation of feedforward inhibition through hippocampal neurogliaform cells. J Neurosci 28:6974–6982. CrossRef Medline

Riven I, Iwanir S, Reuveny E (2006) GIRK channel activation involves a local rearrangement of a preformed G protein channel complex. Neuron 51:561–573. CrossRef Medline

Rüschenschmidt C, Chen J, Becker A, Riazanski V, Beck H (2006) Functional properties and oxidative modulation of A-type K currents in hippocampal granule cells of control and chronically epileptic rats. Eur J Neurosci 23:675–685. CrossRef Medline

Saenz del Burgo L, Cortes R, Mengod G, Zarate J, Echevarria E, Salles J (2008) Distribution and neurochemical characterization of neurons expressing GIRK channels in the rat brain. J Comp Neurol 510:581–606. CrossRef Medline

Saitoh O, Kubo Y, Miyatani Y, Asano T, Nakata H (1997) RGS8 accelerates G protein-mediated modulation of K+ currents. Nature 390:525–529. CrossRef Medline

Scanziani M (2000) GABA spillover activates postsynaptic GABA(B) receptors to control rhythmic hippocampal activity. Neuron 25:673–681. CrossRef Medline

Schmidt-Hieber C, Jonas P, Bischofberger J (2004) Enhanced synaptic plasticity in newly generated granule cells of the adult hippocampus. Nature 429:184–187. CrossRef Medline

Schmidt-Hieber C, Jonas P, Bischofberger J (2007) Subthreshold dendritic signal processing and coincidence detection in dentate gyrus granule cells. J Neurosci 27:8430–8441. CrossRef Medline

Signorini S, Liao YJ, Duncan SA, Jan LY, Stoffel M (1997) Normal cerebellar development but susceptibility to seizures in mice lacking G protein-coupled, inwardly rectifying K+ channel GIRK2. Proc Natl Acad Sci U S A 94:923–927. CrossRef Medline

Sohn JW, Lee D, Cho H, Lim W, Shin HS, Lee SH, Ho WK (2007) Receptor-specific inhibition of GABAB-activated K+ currents by muscarinic and metabotropic glutamate receptors in immature rat hippocampus. J Physiol 580:411–422. CrossRef Medline

Solís JM, Nicoll RA (1992) Pharmacological characterization of $GABA_B$-mediated responses in the CA1 region of the rat hippocampal slice. J Neurosci 12:3466–3472. CrossRef Medline

Spruston N, Johnston D (1992) Perforated patch-clamp analysis of the passive membrane properties of three classes of hippocampal neurons. J Neurophysiol 67:508–529. CrossRef Medline

Staley KJ, Mody I (1992) Shunting of excitatory input to dentate gyrus granule cells by a depolarizing GABAA receptor-mediated postsynaptic conductance. J Neurophysiol 68:197–212. CrossRef Medline

Tamás G, Lorincz A, Simon A, Szabadics J (2003) Identified sources and targets of slow inhibition in the neocortex. Science 299:1902–1905. CrossRef Medline

Tanner GR, Lutas A, Martínez-François JR, Yellen G (2011) Single K ATP channel opening in response to action potential firing in mouse dentate granule neurons. J Neurosci 31:8689–8696. CrossRef Medline

Thompson SM, Haas HL, Gähwiler BH (1992) Comparison of the actions of adenosine at pre- and postsynaptic receptors in the rat hippocampus in vitro. J Physiol 451:347–363. CrossRef Medline

Toni N, Schinder AF (2015) Maturation and functional integration of new granule cells into the adult hippocampus. Cold Spring Harb Perspect Biol 8:a018903. CrossRef Medline

Torrecilla M, Marker CL, Cintora SC, Stoffel M, Williams JT, Wickman K (2002) G protein-gated potassium channels containing Kir3.2 and Kir3.3 subunits mediate the acute inhibitory effects of opioids on locus ceruleus neurons. J Neurosci 22:4328–4334. CrossRef Medline

Treves A, Tashiro A, Witter MP, Moser EI (2008) What is the mammalian dentate gyrus good for? Neuroscience 154:1155–1172. CrossRef Medline

Trussell LO, Jackson MB (1987) Dependence of an adenosine-activated potassium current on a GTP-binding protein in mammalian central neurons. J Neurosci 7:3306–3316. CrossRef Medline

Voigt N, Abu-Taha I, Heijman J, Dobrev D (2014) Constitutive activity of the acetylcholine-activated potassium current IK, ACh in cardiomyocytes. Adv Pharmacol 70:393–409. CrossRef Medline

Wang W, Touhara KK, Weir K, Bean BP, MacKinnon R (2016) Cooperative regulation by G proteins and Na(+) of neuronal GIRK2 K(+) channels. Elife 5:e15751. CrossRef Medline

Wei W, Faria LC, Mody I (2004) Low ethanol concentrations selectively augment the tonic inhibition mediated by δ subunit-containing $GABA_A$ receptors in hippocampal neurons. J Neurosci 24:8379–8382. CrossRef Medline

Wiser O, Qian X, Ehlers M, Ja WW, Roberts RW, Reuveny E, Jan YN, Jan LY (2006) Modulation of basal and receptor-induced GIRK potassium channel activity and neuronal excitability by the mammalian PINS homolog LGN. Neuron 50:561–573. CrossRef Medline

Wydeven N, Marron Fernandez de Velasco E, Du Y, Benneyworth MA, Hearing MC, Fischer RA, Thomas MJ, Weaver CD, Wickman K (2014) Mechanisms underlying the activation of G protein-gated inwardly rectifying K+ (GIRK) channels by the novel anxiolytic drug, ML297. Proc Natl Acad Sci U S A 111:10755–10760. CrossRef Medline

Xie K, Allen KL, Kourrich S, Colón-Saez J, Thomas MJ, Wickman K, Martemyanov KA (2010) Gbeta5 recruits R7 RGS proteins to GIRK channels to regulate the timing of neuronal inhibitory signaling. Nat Neurosci 13:661–663. CrossRef Medline

Yarishkin O, Lee DY, Kim E, Cho CH, Choi JH, Lee CJ, Hwang EM, Park JY (2014) TWIK-1 contributes to the intrinsic excitability of dentate granule cells in mouse hippocampus. Mol Brain 7:80. CrossRef Medline

Young CC, Stegen M, Bernard R, Müller M, Bischofberger J, Veh RW, Haas CA, Wolfart J (2009) Upregulation of inward rectifier K+ (Kir2) channels in dentate gyrus granule cells in temporal lobe epilepsy. J Physiol 587:4213–4233. CrossRef Medline

Zhang Q, Pacheco MA, Doupnik CA (2002) Gating properties of GIRK channels activated by Galpha(o)- and Galpha(i)-coupled muscarinic m2 receptors in *xenopus* oocytes: the role of receptor precoupling in RGS modulation. J Physiol 545:355–373. CrossRef Medline

Zhao S, Zhou Y, Gross J, Miao P, Qiu L, Wang D, Chen Q, Feng G (2010) Fluorescent labeling of newborn dentate granule cells in GAD67-GFP transgenic mice: a genetic tool for the study of adult neurogenesis. PLoS One 5:e12506. CrossRef Medline